2018

Evaluation of the Effect of Scan Strategy on the Accuracy of 4 Intraoral Digital Impression Systems

Jason L. Latham
Medical University of South Carolina

Evaluation of The Effect of Scan Strategy On The Accuracy of 4 Intraoral Digital
Impression Systems

Jason L. Latham, DMD

**A thesis submitted to the faculty of the Medical University of South Carolina in partial
fulfillment of the requirement for the degree of Master of Science in Dentistry in the
College of Dental Medicine**

Department of Orthodontics

Approved by:

Chairman, Advisory Committee

I

Evaluation of The Effect of Scan Strategy On The Accuracy of 4 Intraoral Digital
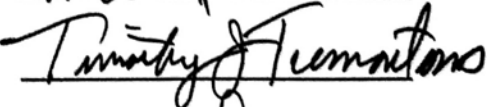Impression Systems

Jason L. Latham, DMD

**A thesis submitted to the faculty of the Medical University of South Carolina in partial
fulfillment of the requirement for the degree of Master of Science in Dentistry in the
College of Dental Medicine**

Department of Orthodontics

Approved by:

Chairman, Advisory Committee

_____

_____

_____

I

TABLE OF CONTENTS

PAGE

LIST OF FIGURES

LIST OF TABLES

<u>Acknowledgements</u>

JASON LEE LATHAM. Evaluation of The Effect of Scan Strategy On The Accuracy of 4 Intraoral Digital Impression Systems (Under the direction of Dr. Wally Renne)

Objective: Digital impression systems, both direct and indirect, are becoming more common in orthodontics. Intraoral scanners (IOS) are devices that are used to directly capture dental impressions. With upgrades and new systems being released at a rapid pace, continued evaluation of device accuracy is essential. This study aims to determine the effects of scan strategy on 4 intraoral digital impression systems.

Materials and Methods: Four digital intraoral impression systems were used to scan a custom made typodont that had a refractive index within the range of enamel and dentin. Four distinct scan patterns, each based off of manufacture suggested patterns, were tested and compared to the reference model. The comparison of test and reference models were completed using an industrial grade metrology software program that allowed both 3D files to be compared for discrepancies. Trueness and precision were then compared for patterns and scanners to determine whether scan pattern affects each. Scan time was also recorded and evaluated for effects on trueness and precision.

Results: Six comparisons were made during this study. Overall scanner comparisons were made, overall patterns were compared, patterns for each scanner were compared, scanners for each pattern were evaluated, maximum deviations

were analyzed, and a visual analysis was completed on the superimposed models. Overall, the trueness ranking was as follows: Element>Trios>Emerald>Omnicam. The Omnicam showed some statistically significant differences in trueness and precision with changes in scan patterns. The Element scan showed statistically significant differences in precision among two of the scan patterns. No statistically significant differences were noted when scan time was evaluated against changes in precision and trueness.

Conclusions: Two of the scanners showed changes in either trueness or precision when scan patterns were altered.   Scan times were not found to affect trueness or precision of the scanners. As new scanners are released, further research is warranted to verify manufacturer claims of accuracy. Although statistically significant differences in trueness and precision were noted between scanners, most showed clinically acceptable accuracy values.

Introduction

Interest in digital scanners has increased dramatically in the market place since its introduction in 1980's with computer aided design and manufacturing (CAD/CAM)[1, 2]. During the near future, intraoral digital scanners could be considered a replacement for traditional alginate and polyvinyl siloxane impressions. Such a change in the method of obtaining impressions would represent a paradigm shift in orthodontics per Kravitz et al[1].

Today, the move toward digital acquisition and storage of orthodontic models is growing rapidly. This transition involves the replacement of plaster models with electronic records to be used for diagnosis, treatment planning, and outcomes assessment. Fabrication of digital models brings several advantages including ease of access to diagnostic information, and a decrease in the need for storage space[3]. Virtual set-ups made from digital models allow for the custom design of removable and fixed appliances[4]. It also provides an easier method to share information with other clinicians, labs and the patient[5].

Currently, there are two methods of obtaining digital impressions: chairside (direct) scans and benchtop (indirect) scans of plaster or gypsum models. Indirect digitization of casts involves scanning casts that were

obtained by traditional impression techniques. This method is often used in laboratory settings, and remains a popular method of digitizing models[6]. A limitation of indirect scanning is the dependence on obtaining alginate or polyvinyl siloxane impressions to fabricate the plaster models that are then scanned.

Direct capture of impressions, which is covered in this study, uses an intraoral scanner (IOS) and offers an alternative by cutting out many of the steps required to obtain traditional or indirect digital model. IOS devices aren't without shortcomings though, with several things potentially affecting their accuracy. Variables such as scanning technology, patient intra-oral blood or saliva, and scanning technique pose potential limitations to IOS accuracy[6, 7].

Accuracy consists of both trueness and precision[8, 9](Figure 1). Trueness is defined as the amount a test object or data set deviates from a reference object or data set. Precision represents the repeatability of measurements. In other words, precision shows how much each test object or data set varies from the last test object[8, 10, 11]. Accuracy of IOS devices has been evaluated using various methods. A large number of studies contain either inter- or intra-arch linear measurements to compare test and reference models. With the help of industrial grade metrology software

programs, accuracy can be assessed using superimposition of test and reference objects.

Accuracy

Trueness

Precision
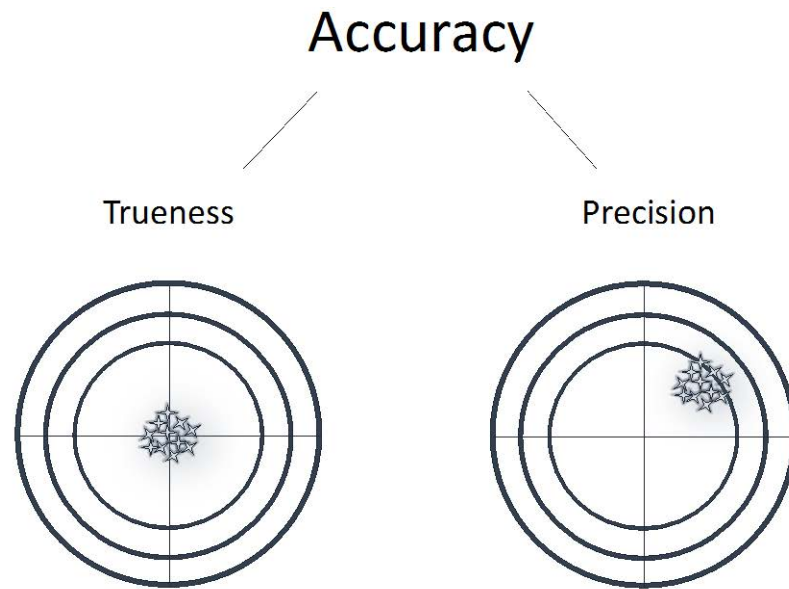
Figure 1. Components of accuracy demonstrated

One of the limitations of previous studies on accuracy includes the assessment of only a portion of the dental arch for accuracy[12-15]. Some authors have found that the more complicated a scan area is, such as a full arch scan, the more that trueness may be affected[16]. This includes studies that evaluated scan pattern changes and their effects on accuracy[10]. Scanning of materials that differ from natural tooth structure may also pose a limitation in accuracy estimation[10, 17-20]. Several studies tested either

metal, or polymeric materials that had a refractive index that may differ from enamel and dentin[6, 9, 11, 12, 21].

Every year new advances in IOS technology are brought to market. As IOS upgrades are made within a practice, doctors and staff may not always adhere to specified manufacture recommended scan patterns while obtaining digital impressions. This could be due to gaps in training, complexity of scan pattern, or limited procedural guidelines set for the office. With the rapid introduction of new technology, regular evaluation must be completed to verify manufacturer claims of accuracy for clinical use, as well as evaluate potential pitfalls that may affect scanner accuracy[7, 22, 23].

This study has a few specific aims. The primary aim of the study is to determine whether scan strategy, or pattern, has an effect on IOS device trueness and precision. A secondary aim is to illustrate whether scan time has any effect on trueness and precision.

The null hypothesis of this study is that scan strategy will not effect trueness or precision, and that scan time will not be related to trueness and precision of the IOS devices tested. The knowledge gained from this research could help clinicians in their use of IOS and scan strategies they choose to use in practice.

Literature Review

History of Dental Impressions

Study model fabrication and evaluation has evolved dramatically from its beginnings in the early 1700's when Phillip Pfaff first described an impression technique utilizing heated sealing wax to create a mold to form models out of Plaster of Paris[24, 25]. Prior to Pfaff's writings, Matthaus Purmann, a surgeon in Germany, described using wax models to duplicate prosthetic devices[25]. One of the first accounts of dental impressions in the United States dates back to a New York Daily advertisement by John Greenwood in 1787. The advertisement stated that artificial teeth could be supplied to individuals who sent in an impression completed in wax[26].

Christophe François Delabarre, a French dentist, described an early impression tray design in 1820. It was noted as a small semi-elliptical track made of metal with a mounted handle. Metal walls, fabricated from white metal or silver, were included to keep buccal tissues away from the softened wax[26].

Calcined plaster was used by Chapin Harris in the late 1830's to fabricate casts from impressions made of wax. Harris wrote in detail regarding the process of obtaining impressions with softened wax, including the use of impression frames used to hold the wax. His method included the

capture of both dental arches simultaneously, then pouring of the plaster one arch at a time[27]. In the 19th century, thermoplastic molding compounds, Plaster of Paris, and gutta-percha were described as various methods of obtaining dental impressions[24].

In the early 1900's, reversible hydrocolloid alginate, followed by irreversible hydrocolloid alginate removed a great deal of shortcomings of previous methods. At the time, alginate proved to be easier to use compared to other options, as well as more dimensionally stable and accurate[24]. Later on, materials such as polyvinylsiloxyane (PVS) and elastic polyether brought more accuracy and dimensional stability[26].

Impregnum was the first polyether material to be specifically used in dentistry. It was introduced by the ESPE company in the mid 1960's[28, 29]. Even with the introduction of more accurate and stable impression materials such as polyether, hydrocolloid alginate currently remains one of the most widely utilized impression materials in orthodontics to this day, along with dental stone that are used to make dental casts[30].

Limitations of Traditional Impressions and Stone Models

Although dental stone casts and alginate have been proven effective in orthodontic record keeping, appliance fabrication, and treatment planning,

they are not without limitations. Alginate has been shown to be affected by some disinfectant methods, and can harbor bacteria if not disinfected properly. Errors in disinfection by staff or clinicians could thus lead to cross contamination in the lab[31]. Several other studies have further shown that inadequate disinfection of impression could yield bacterial transfer to finished dental casts[32, 33].

Voids and bubbles in impressions can yield subsequent models unsatisfactory if they are present in critical areas necessary for appliance fabrication or treatment planning[12]. Various impression materials have been shown to have specific limitations in regards to distortion after a set amount of time. Additionally, the number of casts that can be made from each tray can vary depending on dimensional stability over time, and amount of water absorbed by the impression material[34].

Patient acceptance of conventional impressions as compared to digital alternatives may also play a role in practice. Yuzbasioglu et al evaluated patient responses to conventional impressions compared to digital scans in 2014 and found that patients experienced more discomfort with conventional impressions[35]. In 2015, Burhardt et al surveyed 38 patients in orthodontic treatment on their preferences of impression techniques. The study found that over half of the patients preferred digital impressions,

where as roughly a third of the patients preferred alginate[36]. Hacker et al, in a 2015 survey of 104 dental patients, also reported unpleasant perceptions of impressions from participants[37].

Models made of plaster or stone are prone to breakage. General wear and tear over time, as well as repeated measurements off of the casts can affect accuracy and potentially lead to fracture of the models[30, 38]. Storage presents another problem with traditional storage of stone models. Orthodontic models must be kept various periods, ranging from 5 to 15 years, depending on state laws for patient records[30]. In a busy practice, this could take up a considerable amount of office space, potentially leading to the need for off site storage and increased practice overhead[3, 30].

Stone casts prove difficult to travel with, especially if models are regularly needed for communication between dentists or for patient presentation between multiple offices. The potential for fracture of models while traveling could require duplication of casts[3, 30]. Changes in humidity and temperature over time, as well as exposure to chemicals, can cause distortion to gypsum models[3, 4, 30].

Digital Scanners

The introduction of 3D scanning and computer-aided design/ computer-aided manufacturing (CAD/CAM) in dentistry was reported in the 1980's, but the technology was first used in the 1950's with numerically controlled machines. It was later developed further with the advance of computer software and used a great deal in the automotive and aerospace industries[39]. In the early 1970's, François Duret published his thesis on optical impressions in Lyon, France[4, 40, 41]. He later gained a patent for a CAD/CAM device in 1984[39].

Swiss dentist Werner Mörmann and Marco Bradestini, an electrical engineer, further developed the concept of CAD/ CAM in dentistry[42]. The first commercially available digital scanning system became available to dentistry with the advent of the CEREC system by Sirona Dental Systems in 1987 (Sirona Dental Systems, Besheim, Germany)[41, 42].

Following the introduction of CAD/CAM into dentistry, Cadent (Cadent, Carlestadt, NJ) introduced one of the first orthodontic software programs to the market with OrthoCAD in 1999. Cadent began working on an impression system in 2006 and brought the iTero scanner to market in 2007[1, 39]. This was followed by a variety of systems such as the OrhtoPlex

by Dentsplly GAC, RapidForm by EMS, and Suresmile by Stratos Orametrix[28, 29].

Today, two main types of digital impression systems are available: dedicated digital impression only systems and CAD/CAM systems such as CEREC that can be used to fabricate restorations. Technologies behind each scanner vary, and each system has a manufacturer recommended scan pattern and powdering requirements if needed[28].

Intraoral scanners are designed in accordance with the American National Standards Institute/ International Electrotechnical Commission (ANSI/IEC) standards, specifically 60601-1[1]. Each intraoral scanner can be characterized as having three main parts: a handheld camera, a computer workstation, and a monitor. The handheld camera allows for the digital registration of scan data. Handheld wands vary in capture methods, and technologies behind them vary depending on type of laser or light used. The computer workstation allows for portability around the office, and serves as the point of entry for data. The computer monitor setup can vary, with some systems incorporating it along with the computer, and others supporting separate laptop/ desktop software programs that allow for review of digital scans[1, 41].

Data acquisition is completed via the handheld camera wand in one of two ways: white light or laser light that is emitted from the wand and subsequently reflected back to be captured by a receiving device. The receiving device can be a camera or sensor that is embedded within the wand. Scanners first record x and y coordinates from images or video, the z coordinate calculation varies due to methods on estimating the distance from the sensor to the object[18]. Although a high resolution image is ideal, a great deal of the object's final shape depends on the software algorithms involved in registering data points of interest (POI), which can reach hundreds of thousands of measurements per square inch[1, 3]. Once POI are registered, they are stitched together using algorithms and subsequently compiled into a file, such as a Standard Tessellation Language or Stereolithography (STL) format. Although not discussed here, other file formats such as Polygon File Format (PLY), exist to for object transparency, color, and texture[18].

Each IOS device uses light, whether laser or white light, which can be categorized as either active or passive in the acquisition of data. Active techniques use either blue, white, or red structured light that is projected onto the surface of an object. This technique usually relies less on surface texture and color. With active light techniques, highlighted points on the

object are used to calculate object distance. Another active light method used, and discussed in more detail later, is pattern projection from a light source that is recorded and used to calculate surface coordinates [18, 19]. Passive light techniques use an ambient light source and rely more on surface texture for the registration of data points[18].

Types of IOS Devices

Currently, four main types of technologies are utilized in IOS devices on the market: triangulation, parallel confocal, accordion fringe interferometry (AFI), and three-dimensional motion video, also called 3D motion capture[3].

Triangulation (Figure 2a) is a non-contact scanning technique that uses either active or passive light. It can be divided in as either being active triangulation, or passive triangulation. The system works off the principle that given two points of a triangle, one can calculate the third point and estimate distance from the object. Points can be generated several different ways, such as capturing points a different times, the use of a prism and a single sensor, or the use of multiple sensors[18]. Active triangulation uses a laser light source and directs it onto the surface of an object with a mirror in the scan head. A position sensitive photo-detector and a lens within the

12

camera register the location of the image. The distance from the laser

projector to the camera is known, allowing the point on the object's surface

to be calculated. Instead of using a laser dot to calculate points, IOS systems

can also deploy a series of light projections, such as strip patterns, across the

surface to allow more POI per set amount of time[1, 18, 19]. Passive

triangulation is a technique that uses two cameras, whose distance and

angulation from one another are known allowing distance calculations to be

completed. The technology involved relies on photogrammetric algorithms,

which are used to calculate the distance from two stereo images. This

technique provides high accuracy, but only with highly defined objects. It

lacks ability to precisely distinguish smooth surfaces[19].

Confocal laser scanning microscopy (CLSM) is a non-contact scanning

technique (Figure 2b) that has been around since the early 1960's when

Marvin Minsky first patented the technology. The technique was more

widely adopted by the end of the 1980's[19, 43]. It uses a process known as

optical sectioning and acquires images in-focus from depths that are pre-

selected[44]. This technique allows for a very limited depth of focus,

allowing the system to estimate distance based on the focal length of the lens.

Using successive images taken from a combination of focuses, angles, and

aperture values, objects can be reconstructed using the systems

13

algorithms[18]. The mechanism of action for the scanner involves the

projection of light through an aperture onto the surface of an object, which is

reflected back to the scanner. A specialized pinhole acts as a filter in the

scanner to only allow specific focalized light to pass to the photo sensor,

blocking most out-of-focus light returning from the object[19].

Accordion fringe interferometry (AFI) is a technique that was

developed originally at the Massachusetts Institute of Technology (MIT)

Lincoln Laboratory. It builds on traditional linear laser interferometry

(Figure 3a) by going from 2D analysis to 3D[19]. The technique uses two

projection sources with different fringe patterns that are focused onto an

object. When a fringe pattern hits the surface of an object, it distorts causing

what is known as a "fringe curvature"[1]. The fringe patterns from the

projector are known, so when they are placed on a 3D object the system can

detect distortions caused by surfaces changes. This allows for an accurate

estimation of x, y, and z coordinates, which is recorded for every pixel

captured[19].

Three-dimensional motion capture utilizes a high definition (HD)

camera with three small cameras built within close proximity enabling

trinocular imaging (Figure 3b). This allows the camera to capture views

from three distinct angles. Behind the camera, a complimentary metal-oxide

semiconductor (CMOS) sensor allows for light to be converted into electrical signals[1]. The 3D data is calculated from videos captured from multiple perspectives and modeled in real time[1].
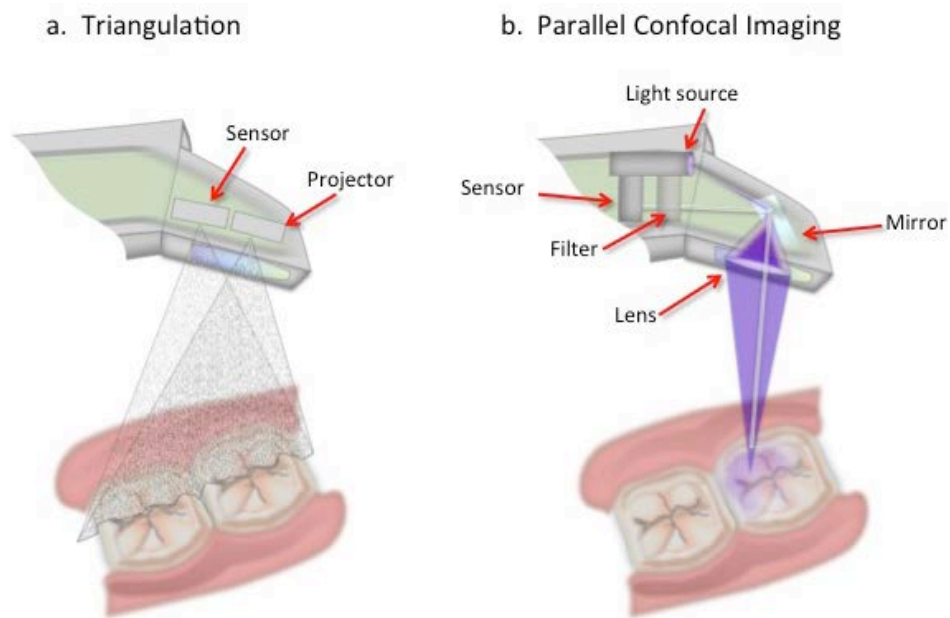
Figure 2. (a), (b). Intraoral scanner examples. **(a)** Triangulation **(b)** Parallel Confocal
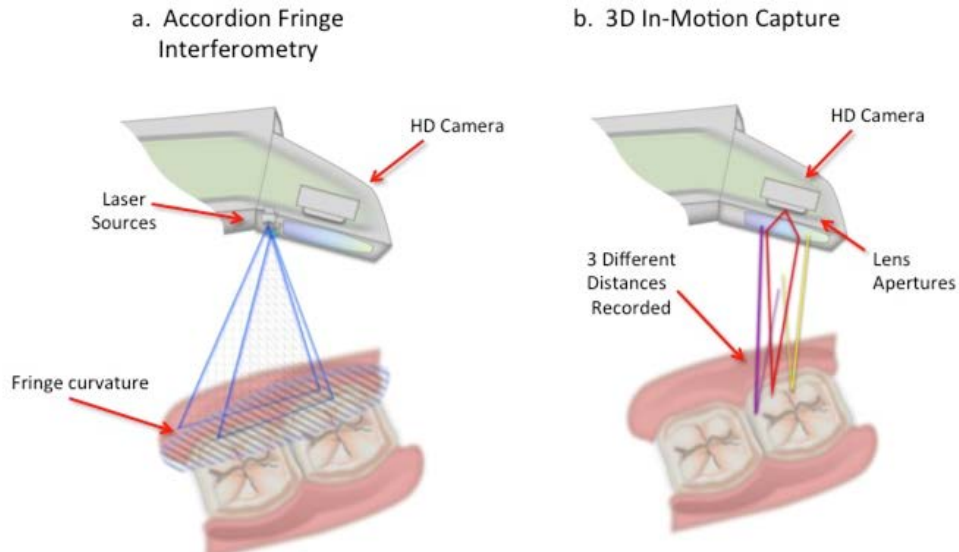
Figure 3 (a), (b). Intraoral scanner examples. **(a)** Accordion Fringe

Interferometry. **(b)** 3D Motion Capture.

Accuracy of IOS

Accuracy, as defined by ISO standards, consists of both trueness and

precision[8, 9](Figure 1). Trueness is defined as the amount a test object or

data set deviates from a reference object or data set. A scanner with higher

trueness delivers a 3D object rendition that most closely matches the

originally scanned object[17]. Precision represents the repeatability of

measurements. In other words, a scanner with higher precision delivers

more consistent results after repeated scans [10].

Accuracy of IOS devices is an important factor when deciding on which scanner to use in a clinical setting. With new scanners emerging rapidly, and new software upgrades changing device algorithms for constructing 3D objects, it is imperative that regular qualitative tests be conducted to verify manufacturer claims. As mentioned previously, a number of articles have been conducted on accuracy, but many only examine a portion of the arch instead of full arch scans[6, 9, 11, 12, 17, 21, 23].

A systematic review conducted by Goracci et al stresses that evidence must be highlighted to verify that IOS impressions are as accurate or more accurate than traditional methods, particularly full arch impressions[23]. They found only a handful of studies assessing validity, repeatability, and reproducibility. Out of their review, it was concluded that current evidence for IOS devices is not up-to-date and not comprehensive enough. This article also pointed out that scan times reported currently vary from study to study, and should be investigated further[23].

A review by Francesco Mangano et al evaluated a number of factors including advantages and disadvantages of IOS devices, whether IOS are as accurate as other means of taking impressions, differences between present day IOS devices, clinical limitations, and potential applications of IOS devices[22]. The review evaluated 132 studies all published over a 10 year

period from 2007 to 2017. Several conclusions were drawn from their

focused questions. Advantages of IOS devices were concluded to be: less

patient discomfort reported, more efficient chairside time, removal of plaster

models, easier communication with clinicians and patients, and simplified

procedures clinically[22]. Several disadvantages were highlighted, including

potentially steep learning curve for staff and clinicians, expense of

purchasing a scanner and management fees, and some difficulty of scanning

margins of prepped teeth. The article covered a number of clinical

indications for IOS devices, including several for orthodontics. The

orthodontic specific indications included diagnosis and treatment planning,

custom made devices and aligners, and creation of virtual records.

Evaluation of accuracy studies from this review showed single tooth or

quadrant impressions to be sufficiently accurate. They also called for a more

critical review of full arch impressions, namely because manufacturers are

releasing devices at a rapid rate, and scientific testing of the devices may be

lagging to verify manufacturer advertised precision and trueness[22].

A separate in vitro study of trueness and precision of four intraoral

scanners by Francesco Mangano et al evaluated full arch scans that included

a fully and partially edentulous maxilla. The study used a powerful reverse

engineering software to superimpose a reference scan and test scans. The

study investigated the Trios 2 (3Shape, Copenhagen, Denmark), CS 3500 (Carestream Health, Rochester, NY, USA), ZFX Intrascan (MHT S.p.A., Verona, Italy), and Planmeca Planscan (E4D Technologies, Richardson, TX, USA). It was found that the systems varied significantly from each other, and highlighted the need for continued investigation.

A systematic review by Vygandas Rutkūnas et al evaluated accuracy of digital implant impressions with IOS devices. Sixteen studies were selected of the 3,661 studies searched. A number of factors were selected that can affect IOS scanner accuracy including hardware, software, experience and performance of the operator, characteristics of object being scanned, clinical factors, and scan strategy[20]. This article highlighted in conclusion that scientific literature is not able to keep up with technological advancements at this time, and ongoing research is necessary.

Several accuracy studies have been conducted on models that may have a refractive index (RI) that varies from enamel and dentin[5, 7, 11, 12, 22, 45, 46]. In a study by Renne et al, a typodont was used with restorations that mimic natural tooth structure[10]. A separate study was conducted using the same typodont by Mennito et al, which further investigated scan strategies[17].

Scan strategy and its effects on IOS accuracy has been evaluated by a limited number of researchers. In a 2013 study, Andreas Ender et al tested three IOS systems using five scanning strategies. The study found that although the IOS devices were capable of high accuracy, close to a previously reported 20.4 μm as seen in conventional PVS impressions, the scan strategy used did have an impact on results[7, 47].

Mennito et al performed a sextant scan study evaluating six IOS devices. In the study, five distinct scan strategies were reviewed and minimal discrepancies were noted between scanners[17]. A study by Philipp Müller et al evaluated full arch maxillary digital impressions using the Trios Pod scanner. Three scan strategies were evaluated from digital scans of a stone model. The study reported a literature review finding that described discrepancies less than 100 μm for a final reconstruction of a 3D model to be clinically acceptable[11, 48]. Müller's investigation found that there were differences in accuracy between the scan patterns tested[11].

Materials and Methods

Overview

Four IOS impression systems were assessed: Planmeca Emerald (PE; Planmeca U.S.A., Roselle, IL), 3Shape Trios 3 color model (TR; 3Shape, Warren, NJ), iTero Element (IE; Align Technology, San Jose, CA), and CEREC Omnicam (CO; Dentsply Sirona, York, PA). Four scan strategies were chosen for this study, each of which selected based on manufacturer recommended patterns. To decrease risk of bias and operator error, each IOS tested was done so by an operator familiar and trained on each particular device.

Scanners Tested

The Planmeca Emerald (PE) was launched in 2017 and is a contact free, powder free IOS system.   It is considered a Class 2 laser scanning device with a wavelength output between 400-700 nm. The model tested was fabricated in February 2018. The scanner utilizes optical triangulation and software algorithms to construct a 3D object from captured live images. The scanner consists of a scanning tip, cable, cradle, and color balancer. It can be connected via USB 3 to a desktop or laptop[49]. Software version 5.9.4 was used for this study.

The 3Shape Trios 3 (TR) is a powder free, contact free IOS that was

released in 2015 and uses using the parallel confocal technology along with

ultrafast optical sectioning[50]. A wireless version was released in 2017, and

the system is offered in either a monochromatic or a color-capturing version.

A USB version for use with a laptop, trolley version including multi touch

screen, and a chairside version are available. Several features are integrated

with some versions including *Real Color Scan*, *Digital Shad Determination*,

and *HD Photo Function*[50]. Model number S1AP was used for this study.

The CEREC Omnicam (CO) impression system is a contact free,

powder free scanner that was released in the summer of 2012. It utilizes

active optical triangulation and active white light to gather POI data[50]. The

system uses video technology allowing for continuous capture of full color,

and allowing tooth shade detection[12]. It is available in either a tabletop

version or a mobile trolley configuration. The CO model tested was equipped

with hardware version 2.24, and software version 4.5.2. After software

version 4.5.1 was released, the CO was opened up to allow direct export of

STL files with the *Open Scan Export* license. All files for this study from the

CO were directly exported from the system.

The iTero Element (IT) is a powder free, contact free system that was

released in 2015. It uses parallel confocal imaging with a red laser beam

light source. An indium tin oxide (ITO) defogging system is used to defog the lens. The manufacturer reports the Element to have an accuracy of roughly less than 20 μm, and is capable of capturing 100,000 points of laser light[51]. Images are captured in full color at a rate of 6,000 frames per second (FPS). According to the manufacturer, the scan wand houses built-in controls, and an integrated gyro technology allows the user to adjust views of 3D models on the screen. The system comes with an optional wheel stand or stationary countertop stand, scan wand, and multi touch 19-inch screen integrated with the computer[52]. Software version 1.5.0.361 was used for this study.

Master Model Fabrication

A master scan was used as a reference to evaluate accuracy and precision. The customized master model used for the reference was fabricated using a maxillary dentiform model (Kilgore Intl Inc) with fourteen maxillary typodont teeth (Model D85SDP-200; Nissin Dental Products Inc). Each typodont tooth was prepared for full coverage ceramic crowns in compliance with guidelines from Rosenstiel et al [53] with a continuous 1 mm modified shoulder finish line that follows the free gingival margin, 1-1.5 mm axial surface reduction, 1.5-2 mm occlusal reduction with a

functional cusp bevel, and between 6-10 degrees of taper[53]. All surfaces were further finished for an overall rounded and smooth finish.

Restorations were completed with Telio CAD (TC) polymethyl methacrylate (Ivoclar Vivadent AG) in shade A3. The TC composite has a refractive index of 1.49, which is similar to dentin (1.54) and enamel (1.63), thus enabling a closer simulation to natural tooth substance[10, 17]. Prior to bonding, the intaglio surfaces of the restorations were air abraded with 40µm CoJet sand (3M ESPE). Cementation of the restorations was completed with Rely-X Unicem (3M ESPE), a self-etching, self-adhesive resin cement.

A master scan of the model was made using an industrial scanning company (Capture 3D, Santa Ana, CA), and was used as a reference for trueness and precision testing against experimental scans. The master scan was attained using an ATOS III Triple Scan 3D optical scanner (GOM, Braunschweig, Germany). The ATOS is a non-contact structured blue-light scanner that works by using multiple cameras that record a course of stripes projected on an object being measured. For each pixel of the camera sensor's points, coordinates can be estimated with very high precision[54]. For jaw sized scans, this scanner has shown accuracy of 3 µm and precision of 2 µm[55].

Experimental Scans

A series of experimental scans were obtained from each of the IOS systems. A recent study by Lim et al investigated the effect of repetitive operator experience on trueness and precision and noted that some scanning system accuracy measurements could potentially be effected by operator experience. Although less likely in video scanning systems as compared to single-image scanning systems, some changes in accuracy were noted[56]. This study selected operators experienced and extensively trained in each IOS system as to minimize risk of inaccurate trueness and precision measurements due to user experience.

Four experimental scans were obtained from each of the scanners using distinct scan strategies. Scan patterns (SP) 1-4 were based off of PE, IE, TR, and CO operator manuals. For each scan performed, both scan time and rendering time were recorded.
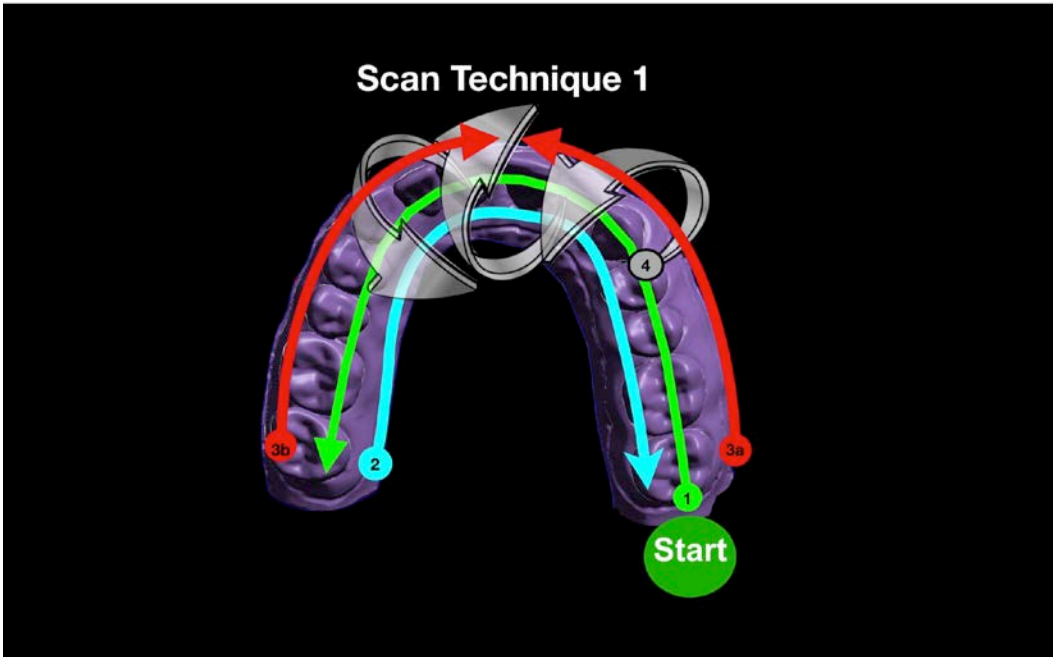
Figure 4. SP1 scan technique.

Scan pattern 1 (SP1, Figure 4) began on the second molar and all occlusal surfaces were captured until the contralateral second molar was reached. Once the second molar was reached. A lingual role was then performed and the remaining lingual surfaces were captured until the opposite second molar was reached. To capture the buccal surfaces, a two-part technique was used step 3a and 3b. First the buccal surfaces were captured from the left second molar until the midline was reached, then the buccal surfaces were captured from the right second molar until the midline was reached. The scan was completed with a lingual to buccal role from cuspid to cuspid.

26
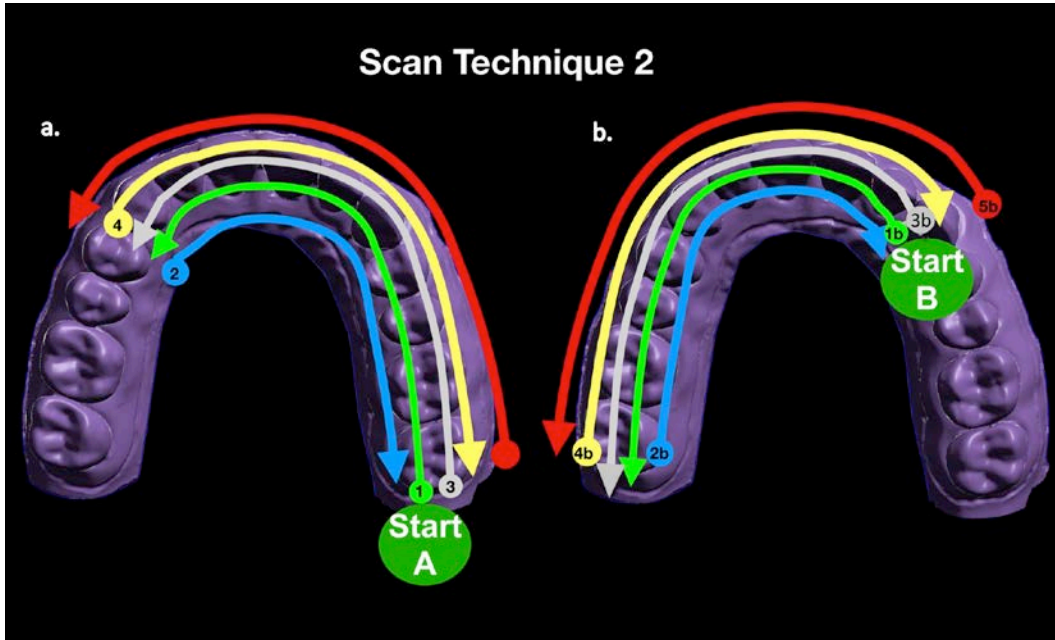
Figure 5 (a), and (b). SP2 scan technique. **(a)** Scan pattern shown starting at terminal molar. **(b)** Second portion of scan pattern shown.

Scan Pattern 2 (SP2, Figure 5) involved 2 parts, each containing 5 separate steps. It began at the occlusal surface of the terminal molar, where a lingual role was performed and lingual surfaces were captured at an angle of 45° to the occlusal surface (Figure 5a). Once the contralateral premolar was reached, the scan head was rolled so that the lingual surfaces could be captured at a 90° angle to the occlusal surface in a direction back to the initial starting molar. The occlusal surface was then captured from the molar to the contralateral premolar, and the scanner was rotated to capture the buccal surfaces at an angle 45°to the occlusal surface. Once the buccal surfaces were captured, the scanner was rotated so that the buccal surfaces could be

captured at an angle of 90°to the occlusal surfaces. A similar pattern was

then used (Figure 5b.) to capture the remaining portion of the arch. It

started from the premolar residing on the initially scanned side, and began

by scanning lingual at a 45° angle to the occlusal surface of the premolar and

progressing to the un-scanned terminal molar. There the scanner was then

rotated 90°to the occlusal plane and lingual surfaces were captured back to

the premolar. Next, while at the premolar, the occlusal surfaces were

captured, followed by buccal surfaces at a 45° angle to the occlusal surfaces.

Buccal surfaces were then captured at a 90° angle to the occlusal surface

finishing at the premolar.
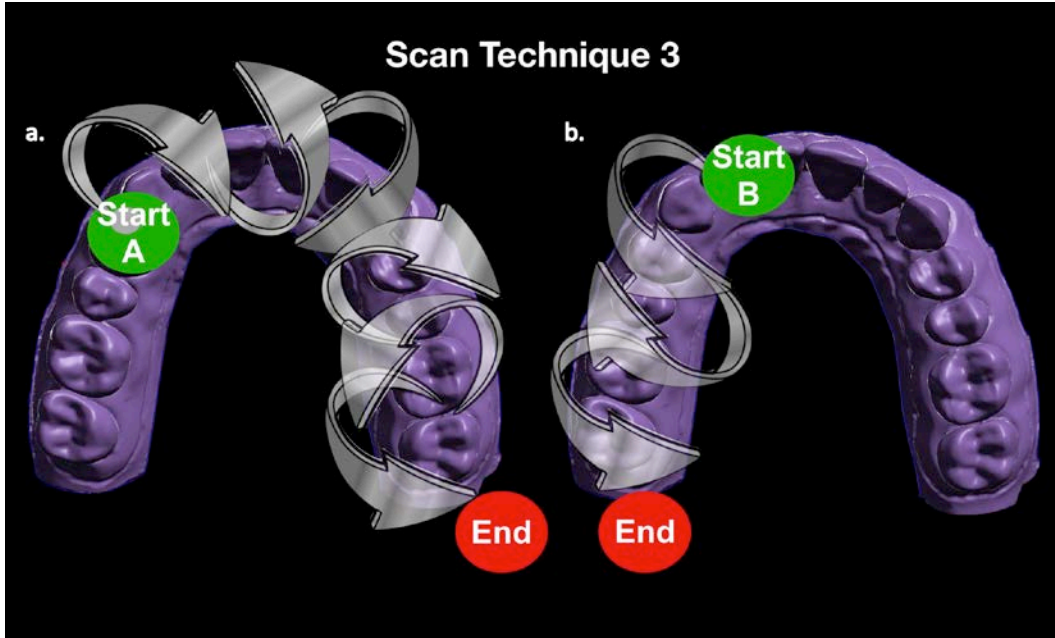
Figure 6 (a), and (b). SP3 scan technique. **(a)** Scan pattern starting at cuspid. **(b)** Second portion of scan pattern illustrated.

Scan pattern 3 (SP3, Figure 6) began at the right cuspid and a lingual to buccal role was completed on each tooth until the left second molar was reach. The scan was picked back up at the initial cuspid, and the same lingual to buccal role completed to the right second molar.
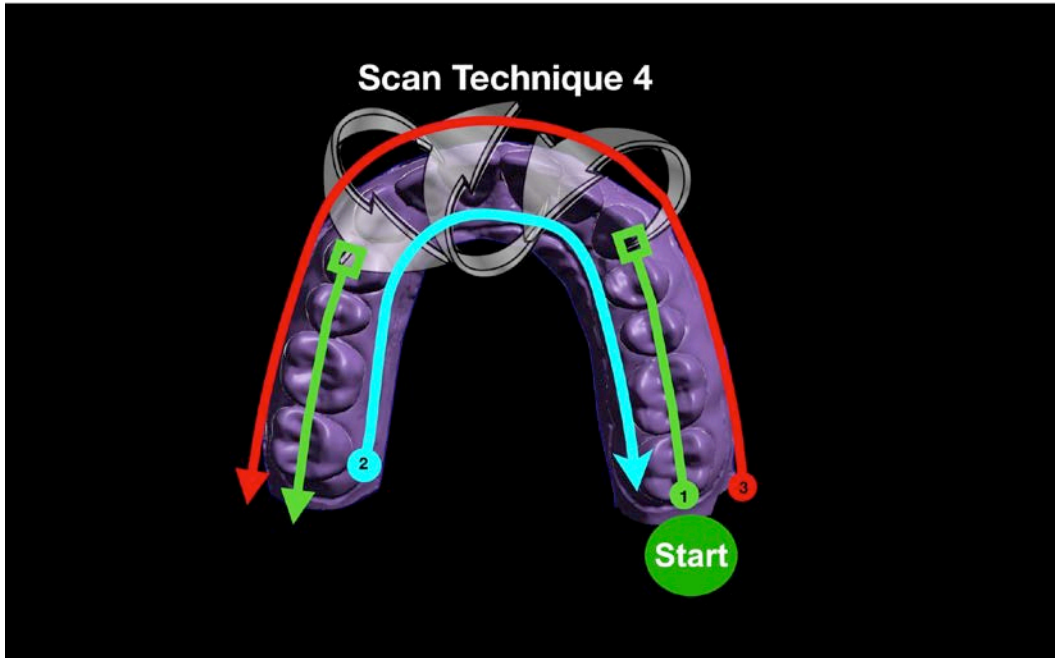
Figure 7. SP4 scan technique illustrated.

Scan Pattern 4 (SP4, Figure 7) began at the terminal molar, capturing occlusal surfaces until the cuspid was reached. From cuspid to contralateral cuspid, a buccal to lingual role was performed on each tooth. Resuming at the premolar, occlusal surfaces were captured until the terminal molar was reached. Next the scanner was rotated to the lingual and all lingual surfaces captured, followed by all buccal surfaces.

3D Analysis

All experimental scans were converted to stereolithography (STL) format utilizing the appropriate manufacturers recommended conversion method. A comprehensive metrology program, Geomagic Control X (3D Systems, Rock Hill, South Carolina), was used to compare the master model with the experimental STL files.

Once imported into the software, models were digitally trimmed along a reference line made on the original solid model using the software's trim function (Figure 8). Once models were trimmed, the reference model STL file was imported and trimmed on the opposite side of the original reference line to ensure adequate test model overlap (Figure 9).
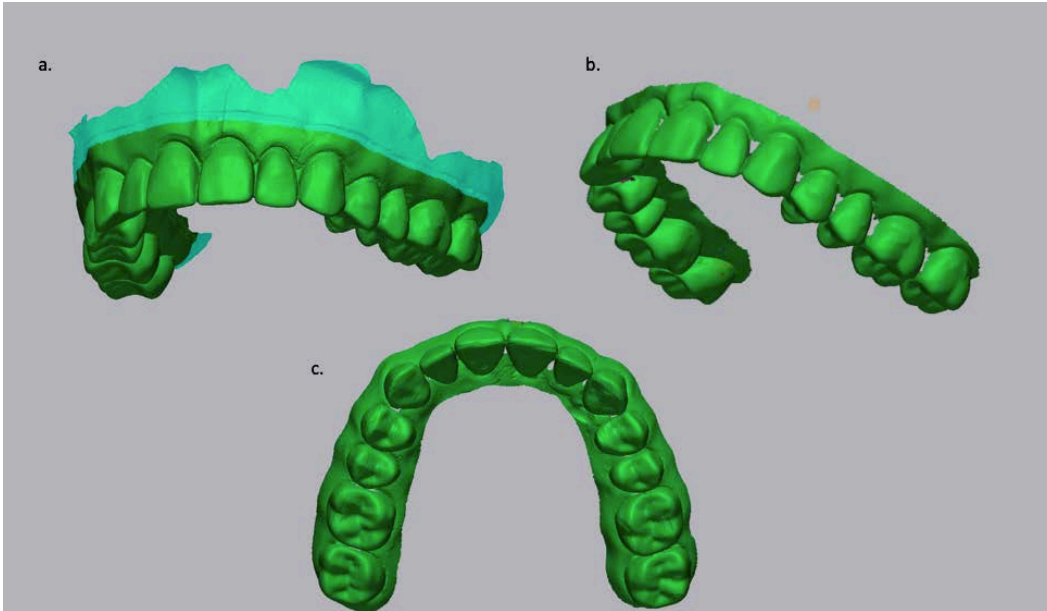
Figure 8. (a), (b), and (c). Imported experimental models in green. **(a)** Untrimmed model. Areas highlighted in light green were removed from the model. **(b)** Oblique view of trimmed test model, including interproximal surfaces which were removed digitally. Axial cut was completed along a premade reference line. **(c)** Occlusal view of trimmed test model prior to alignment with reference model.
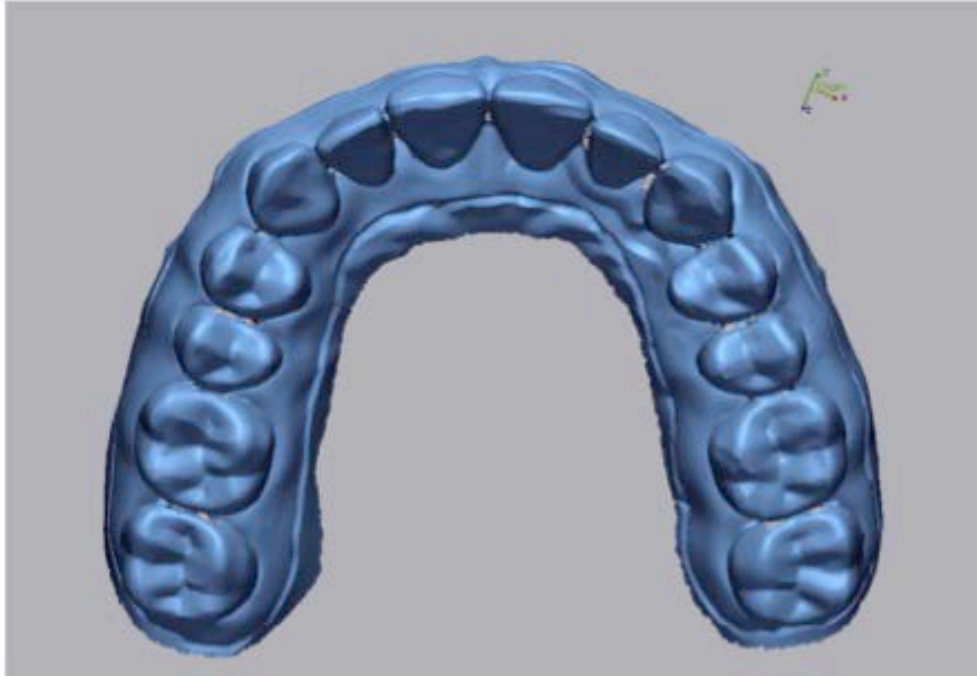
Figure 9. Trimmed reference model highlighted in blue. Axial cut made superior to reference line.

Using Geomagic's *Initial Alignment* and *Best Fit Alignment* functions, models were overlaid in preparation for 3D comparisons (Figure 10). The software's *Best Fit Alignment* function acts to align the test file and reference file using an iterative closest point algorithm (ICP). Originally introduced by Chen and Medioni in 1991, and McKay and Besl in 1992, ICP has become one of the mostly widely adopted methods for aligning digital 3D files[57]. It is a data driven approach that uses point cloud properties to aid in aligning 3D objects. The algorithm uses 3D correspondences between two clouds of points and determines the minimal distance between objects[58]. Per the

33

manufacturer, the objects are first brought into a relative aligned position

using Geomagic's algorithms. The software then evaluates the test file, and

the points that are the closest are computed on the reference file. The

resulting overlay shows the reference model in a new grey color, and the test

model remains in green.
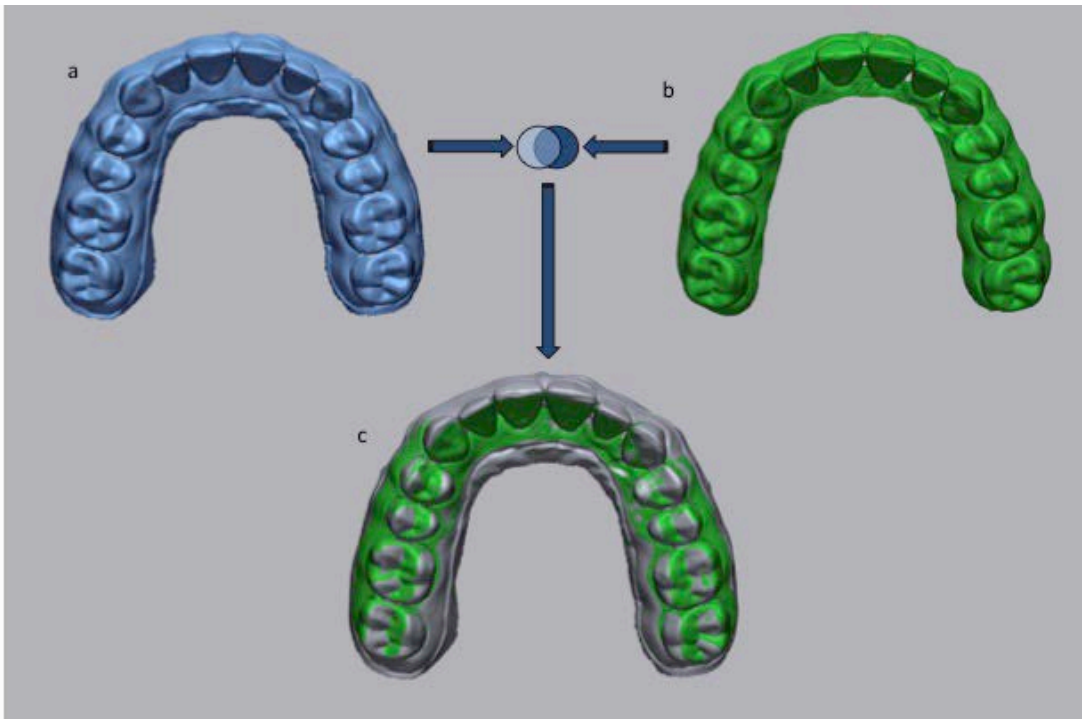
Figure 10. (a), (b), and (c). Software *Best Fit Alignment* demonstrated. **(a)** Trimmed reference model in blue. **(b)** Trimmed test model in green. **(c)** Reference and test model overlaid after superimposition completed.

The software's *3D Compare* function allows for customization of measurements and color mapping of results. A value of 0.5mm was used to define upper and lower limits for color mapping (Figure 11). No reference tolerances were set for this study, and color mapping was chosen to display deviations on the digital models (Figure 12). Models displayed after the completion of the 3D Compare function showed a range of colors that correlated with potential areas of mismatch between the test and reference model. Darker blue highlighted areas indicated a negative or inward deviation, and darker red highlighted areas indicated a positive or outward deviation of the test model. Reports were generated for each comparison and values for average, minimum deviation, maximum deviation, and standard deviation were compiled in an excel spreadsheet (Figure 13).
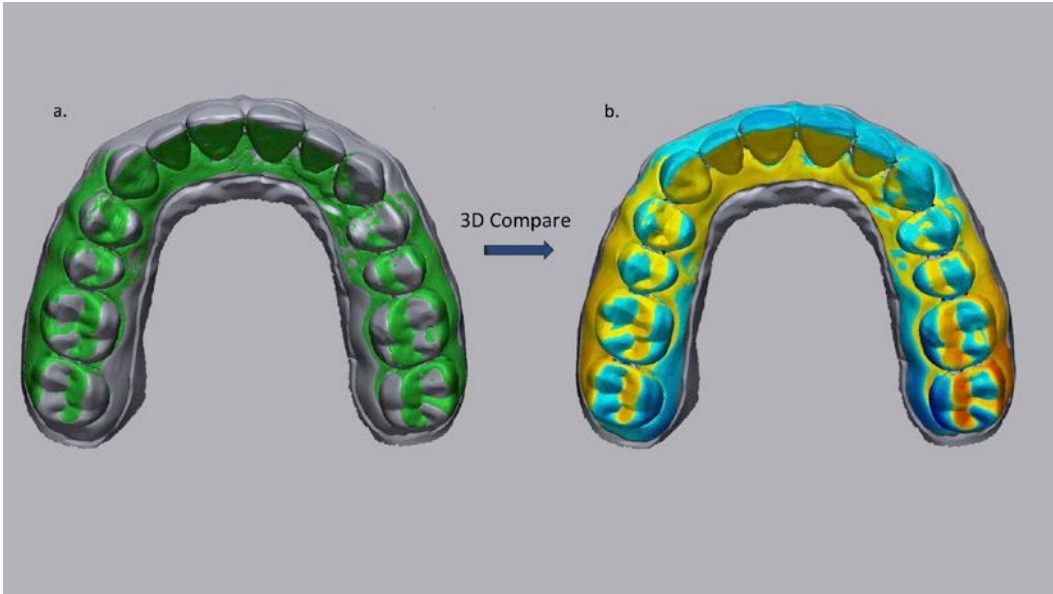
Figure 11. (a) and (b). **(a)** Initial superimposition. **(b)** 3D Compare with color to indicate discrepancies.
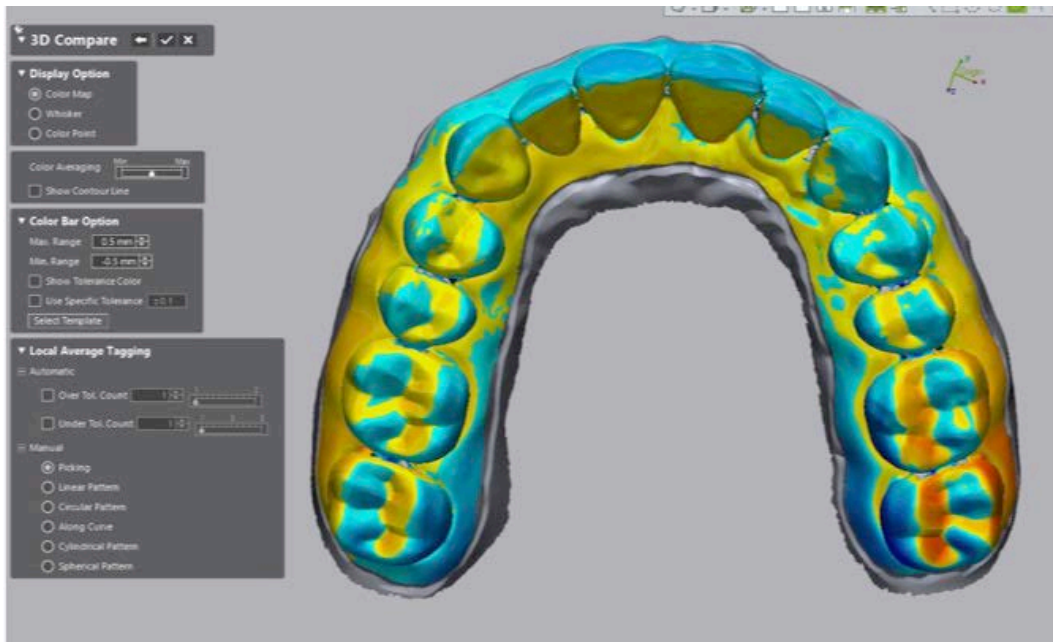
Figure 12. 3D Compare settings on left: color map option used with minimum and maximum color deviations set at 0.5 mm.

Min.	-0.3816
Max.	0.3819
Avg.	-0.0195
RMS	0.0715
Std. Dev.	0.0687
Var.	0.0047
+Avg.	0.038
-Avg.	-0.0602
In Tol.(%)	99.475
Out Tol.(%)	0.525
Over Tol.(%)	0.049
Under Tol.(%)	0.476
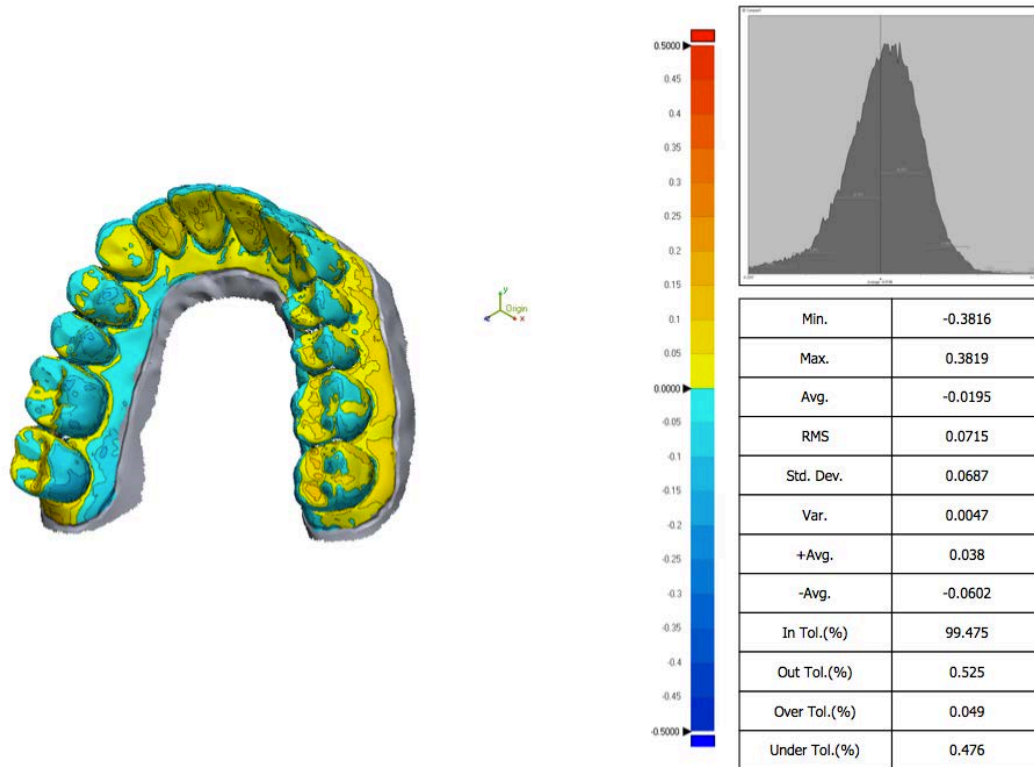
Figure 13. Color map shown on the right indicating red for positive deviations and blue for negative deviations.

<u>**Results**</u>

        Scanners were first evaluated overall for trueness, precision, and time

averages. This included all 16 scans performed for each IOS device. The

scanners were then compared in two main ways: Scan patterns within each

scanner, and scanners within each scan pattern. Minimum and maximum

deviation values were analyzed by adding their absolute values and taking a

mean value. The results were assessed for statistical differences and

compared to those of pattern and scanner trueness. Finally, the *3D Compare*

outputs from the Geomagic Control X reports were assessed for changes in

color, which indicates deviations from the test and reference models.

Overall Scanner Comparisons

Table 1. Overall scanner comparisons including trueness and precision in
microns, and scan time in minute format.

Scanner	Trueness (Avg)	Trueness Rank	Precision (Std)	Precision Rank	Scan Time (Avg)	Scan Time Rank
Element	46	1	17	2	3.30	4
Emerald	59	3	8	1	2.12	3
Omnicam	119	4	38	4	2.06	2
Trios	47	2	22	3	1.39	1

Overall Trueness (Average)

A repeated measures generalized linear model was used with average deviation as the outcome and scanner in the model. A random intercept was in the model to account for replicates. Scanner was found to be significant ($p<0.0001$) so the post hoc pairwise comparisons were looked at with a Scheffe adjustment. The significant comparisons were IE vs PE (p-value=0.0183), IE vs CO (p-value=<0.0001), EM vs CO (p-value=(0.0001), TR vs PE (p-value=0.0370), TR vs CO (p-value=<0.0001). Significant differences in overall scanner trueness are listed in Table 2. Scanners with higher trueness are listed on the left.

Table 2. Significant differences in complete arch trueness. Scanners with higher trueness on left.

Scanner		Scanner	P-value
Element	vs	Emerald	0.0183
Element	vs	Omnicam	<.0001
Emerald	vs	Omnicam	<.0001
Trios	vs	Emerald	0.0370
Trios	vs	Omnicam	<.0001

Overall Scanner Trueness (μm)
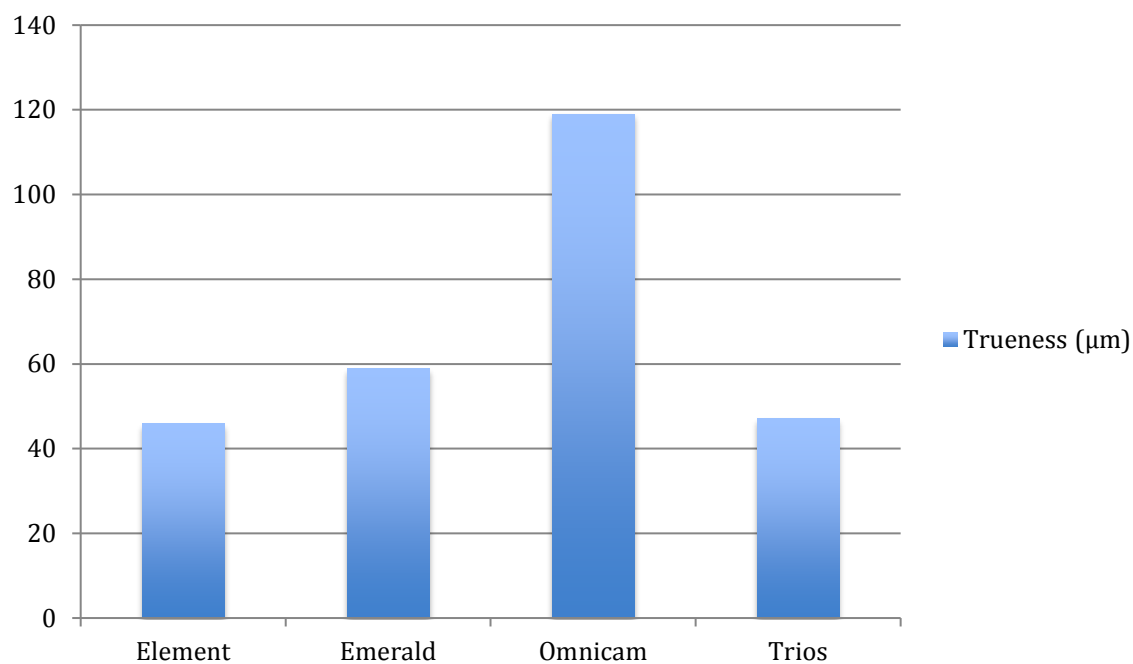
Figure 14. Overall scanner trueness including all scan patterns. Inter-system variations were found to be significantly different between all scanners except the IE and TR devices.

Overall Scanner Precision

A repeated measures generalized linear model was used with average deviation as the outcome and scanner in the model. A random intercept was in the model to account for replicates. Scanner was found to be significant ($p<0.0001$) so the post hoc pairwise comparisons were looked at with a Scheffe adjustment. The significant comparisons are listed in Table 3 with higher precision scanners on the left.

Table 3. Significant differences in complete arch precision. Scanners with higher precision on left.

Scanner		Scanner	P-value
Element	vs	Emerald	<.0001
Element	vs	Omnicam	<.0001
Trios	vs	Element	0.0044
Emerald	vs	Omnicam	<.0001
Trios	vs	Emerald	<.0001
Trios	vs	Omnicam	<.0001

Overall Scanner Precision (Std Dev)
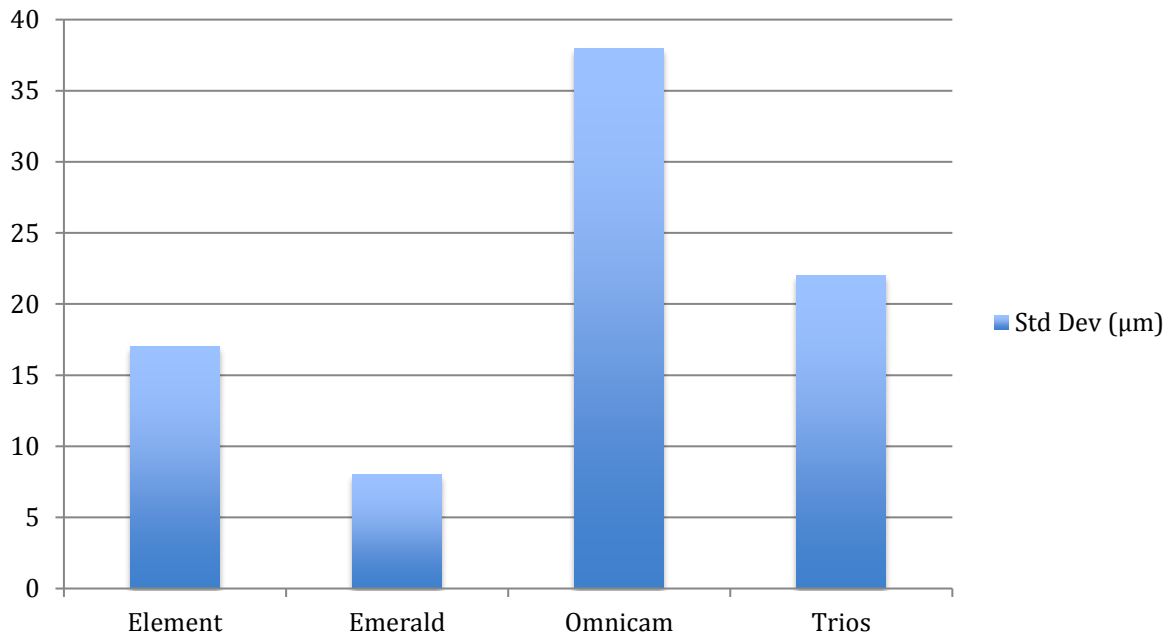
Figure 15. Overall scanner precision including all scan patterns. Inter-system variations were found to be significantly different between all scanners.

Overall Device Scan Times

A repeated measures generalized linear model was used with scan time as the outcome and scanner in the model. A random intercept was in the model to account for replicates. Scanner was found to be significant (p<0.0001) so the post hoc pairwise comparisons were looked at with a Scheffe adjustment. IE vs PE (p-value<0.0001), IE vs CO (p-value<0.0001), IE vs TR (p-value<0.0001), IE vs TR (p-value=0.0007) and CO vs TR (p-value=0.0019) were all statistically significant. PE vs CO (p-value=0.9911)

was not significant. Post-hoc comparisons are listed in Table 4. Additionally,

scan time and scanner trueness were set as covariants and not found to be

significant (p-value=0.7344). Scan time and scanner precision were set as

covariants and were not found to be significant (p-value=0.3615).

Table 4. Overall scanner times post-hoc comparisons. Scanners with shorter scan times are listed on the left.

Overall Scan Times

Scanner		Scanner	P-value
Emerald	vs	Element	<0.0001
Omnicam	vs	Element	<0.0001
Trios	vs	Element	<0.0001
Trios	vs	Emerald	0.0007
Trios	vs	Omnicam	0.0019

Overall IOS Device Scan Times
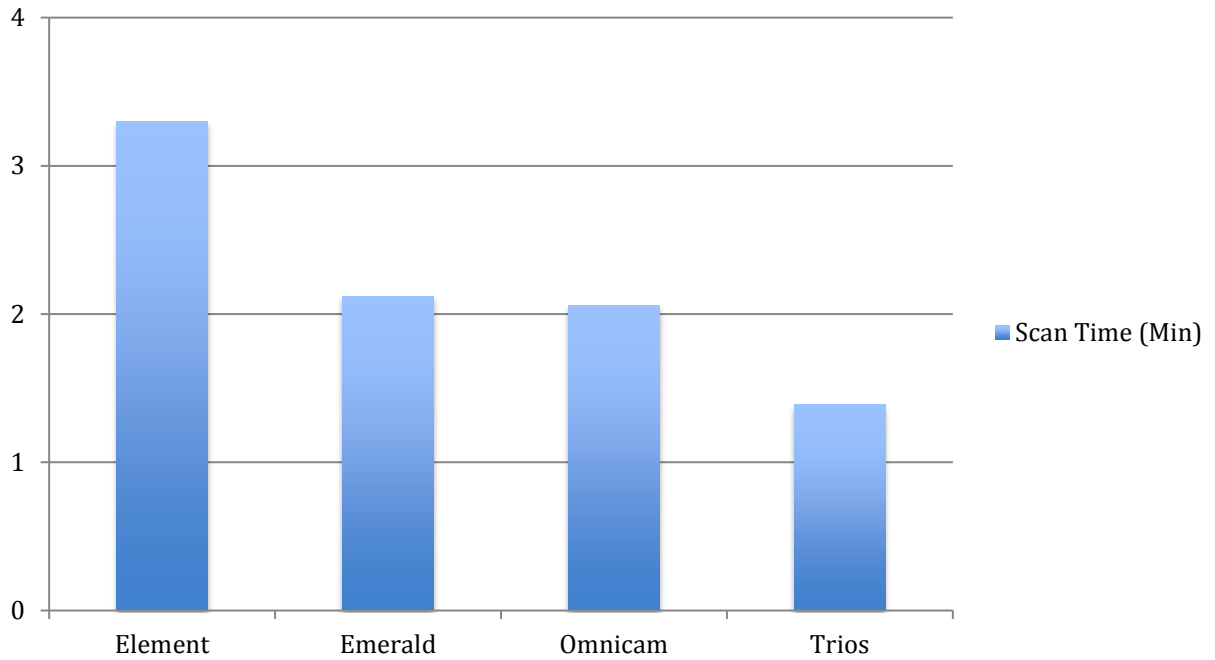
Figure 16. Overall scanner time averages. Each scanner shown includes averages for all scan pattern times within each scanner.   Inter-system variations were found to be significantly different for all scanners except the PE vs CO.

Overall Scan Pattern Comparisons

Table 5. Overall scan pattern comparisons including trueness and precision in microns, and scan time in minute format.

Scan Pattern	N	Trueness (Avg)	Trueness Rank	Precision (Std)	Precision Rank	Scan Time (Avg)	Scan Time Rank
1	16	70.5	2	23	4	2.27	3
2	16	60	1	18	1	2.09	2
3	16	71.5	4	21	2	2.60	4
4	16	71	3	22	3	1.91	1

Overall Scan Pattern Trueness

A repeated measures generalized linear model was used with average deviation as the outcome and scanner in the model. A random intercept was in the model to account for replicates. Scan pattern was found to be not significant (p-value= 0.7365).

Figure 17. Overall scan pattern trueness compared. Each scan pattern illustrated includes trueness averages from all scanners used for that particular pattern. No significant differences present (p-value=0.7365).

Overall Scan Pattern Precision

A repeated measures generalized linear model was used with precision as the outcome and scanner in the model. A random intercept was in the model to account for replicates. Scanner pattern precision was found to be not significant (p-value=0.6587).
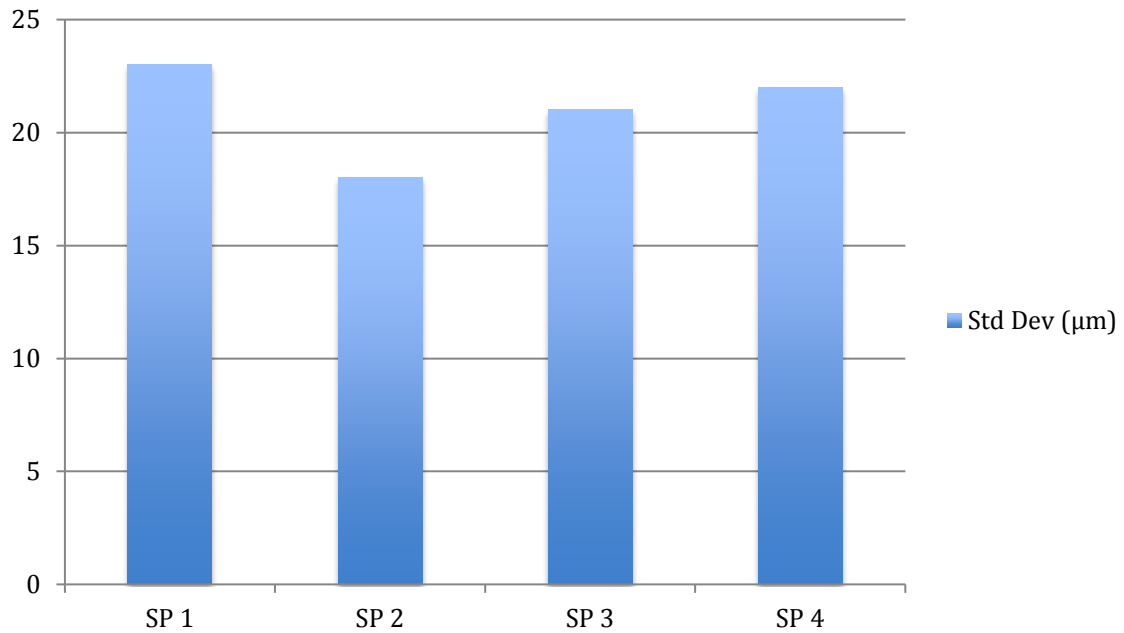
Figure 18. Overall scanner precision including all scanners. No significant differences noted between scan pattern precision values.

Overall Scan Pattern Times

A repeated measures generalized linear model was used with scan time as the outcome and scanner in the model. A random intercept was in the model to account for replicates. Scanner was found to be not significant (p-value=0.0987).

Overall Pattern Scan Times
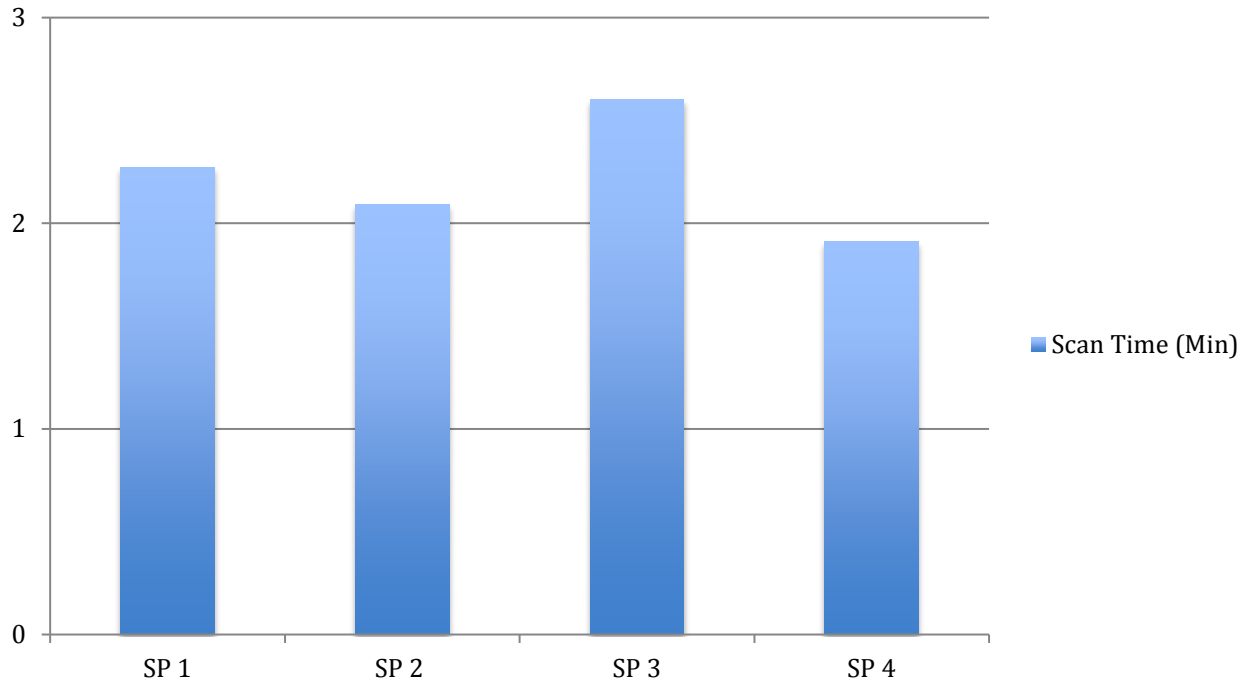
Figure 19. Overall scan pattern time averages. No significant differences were noted between scan pattern times (p-value=0.0987)

Scan Pattern Comparisons Within Each Scanner

Table 6. Scan patterns are compared within each scanner including trueness and precision in microns, and scan time in minute format.

Scanner	Pattern	N	Trueness (Avg)	Trueness Rank (within Scanner)	Precision (STD)	Precision Rank (within Scanner)	Scan Time (Min.Sec)	Scan Time Rank (within Scanner)
Element	1	4	44	1	18	4	3.70	4
	2	4	50	4	17	3	3.33	2
	3	4	46	3	16	2	3.44	3
	4	4	45	2	15	1	2.74	1
Emerald	1	4	67	3	11	4	2.16	3
	2	4	49	1	5	2	1.66	2
	3	4	55	2	4	1	3.20	4
	4	4	69	4	10	3	1.45	1
Omnicam	1	4	122	2	42	3	1.82	1
	2	4	93	1	30	1	2.05	2
	3	4	138	4	42	3	2.33	4
	4	4	124	3	41	2	2.05	2
Trios	1	4	49	4	22	2	1.41	3
	2	4	48	3	21	1	1.32	1
	3	4	47	2	23	4	1.45	4
	4	4	46	1	21	1	1.38	2

Comparing Trueness of scan patterns for each scanner

The main effect for IE was not significant (p-value=0.5500) or for PE (p-value=0.1236) or for TR (p-value=0.7796). For CO it was significant (p-value=0.0019) and the significant comparisons are shown below.

Table 7. Significant trueness differences of scan strategies within Omnicam scanner. Patterns with higher trueness are on the left.

Omnicam Scanner

Pattern		Pattern	P-value
SP 2	vs	SP 1	0.0303
SP 2	vs	SP 3	0.0023
SP 2	vs	SP 4	0.0248

Precision of Scan Patterns for Each Scanner

For IE the main effect was significant (p-value=0.0307) and Pattern 1 vs 4 was (p-value=0.0345). For PE the main effect was not significant (p-value=0.0535). For CO the main effect was significant (p-value=0.0026) and Pattern 1 vs 2 (p-value=0.0069), Pattern 2 vs 3 (p-value=0.0099) and Pattern 2 vs 4 (p-value=0.0150) were significant. The main effect for TR was not significant (p-value=0.5250). The precision significant differences of scan patterns within scanners are listed in Table 8.

Table 8. Significant differences among precision values from scan patterns within the IE and CO scanners. Patterns with higher precision are on the left.

Element Scanner

Pattern		Pattern	P-value
SP 4	vs	SP 1	0.0345

Omnicam Scanner

Pattern		Pattern	P-value
SP 2	vs	SP 1	0.0069
SP 2	vs	SP 3	0.0099
SP 2	vs	SP 4	0.0150

Scan Time From Scan Patterns Within Each Scanner

A repeated measures generalized linear model was used with scan time as the outcome and s in the model. Four models were run, one for each scanner. A random intercept was in the model to account for replicates. Post hoc comparisons for pattern with a Scheffe adjustment were looked at if the main effect was significant.

IE (p-value=0.0331) had a significant main effects for pattern. Pattern 1 vs 4 (p-value=0.0396) was statistically significantly different. PE (p-value<0.001) also had a significant main effects for pattern. Pattern 1 vs 2 (p-value=0.0089), Pattern 1 vs Pattern 3 (p-value<0.0001), Pattern 1 vs 4 (p-value=0.0008), Pattern 2 vs 3 (p-value<0.0001) and Pattern 3 vs 4 (p-value<0.001) were all statistically significant. CO (p-value=0.0564) was also

marginally significant. The only comparison that was marginally significant

was Pattern 1 vs 3 (p-value=0.0573).

Table 9. Significant differences among scan times from patterns within the scanners. Shorter scan times are listed on the left side of the table.

Element Scanner

Pattern		Pattern	P-value
SP 4	vs	SP 1	0.0396

Emerald Scanner

Pattern		Pattern	P-value
SP 2	vs	SP 1	0.0089
SP 1	vs	SP 3	<0.0001
SP 4	vs	SP 1	0.0008
SP 2	vs	SP 3	<0.0001
SP 4	vs	SP 3	<0.0001

Omnicam Scanner

Pattern		Pattern	P-value
SP 1	vs	SP 3	0.0573

Scanners Within Scan Patterns

Table 10. Scanners are compared within each scan pattern.

Pattern	Scanner	N	Trueness (average)	Trueness Rank (within Scanner)	Precision (STD)	Precision Rank (within Scanner)	Scan Time	Scan Time Rank (within Scanner)
SP 1	Element	4	44	1	18	4	3.70	4
	Emerald	4	67	3	11	3	3.33	2
	Omnicam	4	122	4	42	2	3.44	3
	Trios	4	49	2	22	1	2.74	1
SP 2	Element	4	50	4	17	2	2.16	3
	Emerald	4	49	2	5	1	1.66	2
	Omnicam	4	93	4	30	3	3.20	4
	Trios	4	48	1	21	2	1.45	1
SP 3	Element	4	46	1	16	2	1.82	1
	Emerald	4	55	3	4	1	2.05	2
	Omnicam	4	138	4	42	4	2.33	4
	Trios	4	47	2	23	3	2.05	2
SP 4	Element	4	45	1	15	2	1.41	3
	Emerald	4	69	3	10	1	1.32	1
	Omnicam	4	124	4	41	4	1.45	4
	Trios	4	46	2	21	3	1.38	2

Trueness of Scanners Within Scan Patterns

A repeated measures generalized linear model was used with trueness as the outcome and scanner in the model. Four models were run, one for each pattern. A random intercept was in the model to account for replicates. Post hoc comparisons for scanner with a Scheffe adjustment were looked at if the main effect was significant. For Pattern 1, the main effect was significant (p-value<0.0001), and the post-hoc comparisons of IE vs CO (p-value<0.0001), PE vs CO (p-value=0.0002) and CO vs TR (p-value<0.0001) were all significant. The main effect for Pattern 2 was significant (p-value<0.0001), as were the post-hoc comparisons of IE vs CO (p-value=0.0002), PE vs CO (p-value=0.0002) and CO vs TR (p-value=0.0002). The main effect for Pattern 3 was significant (p-value<0.0001), as were the post-hoc comparisons for IE vs CO (p-value<0.0001), PE vs CO (p-value<0.0001) and CO vs TR (p-value<0.0001). The main effect for Pattern 4 was significant (p-value<0.0001), as were the post-hoc comparisons for IE vs PE (p-value=0.0274)), IE vs CO (p-value<0.0001), PE vs CO (p-value<0.0001), PE vs TR (p-value=0.0343), and CO vs TR (p-value<0.0001).

Table 11. Trueness significant differences among scanners within scan patterns. Scanners with higher trueness are listed on the left.

Scan Pattern 1

Scanner		Scanner	P-value
Element	vs	Omnicam	<0. 0001
Emerald	vs	Omnicam	0.0002
Trios	vs	Omnicam	<0. 0001

Scan Pattern 2

Scanner		Scanner	P-value
Element	vs	Omnicam	0.0002
Emerald	vs	Omnicam	0.0002
Trios	vs	Omnicam	0.0002

Scan Pattern 3

Scanner		Scanner	P-value
Element	vs	Omnicam	<0. 0001
Emerald	vs	Omnicam	<0.0001
Trios	vs	Omnicam	<0. 0001

Scan Pattern 4

Scanner		Scanner	P-value
Element	vs	Omnicam	<0. 0001
Element	vs	Emerald	<0. 0274
Emerald	vs	Omnicam	<0. 0001
Trios	vs	Emerald	<0. 0001
Trios	vs	Omnicam	<0. 0001
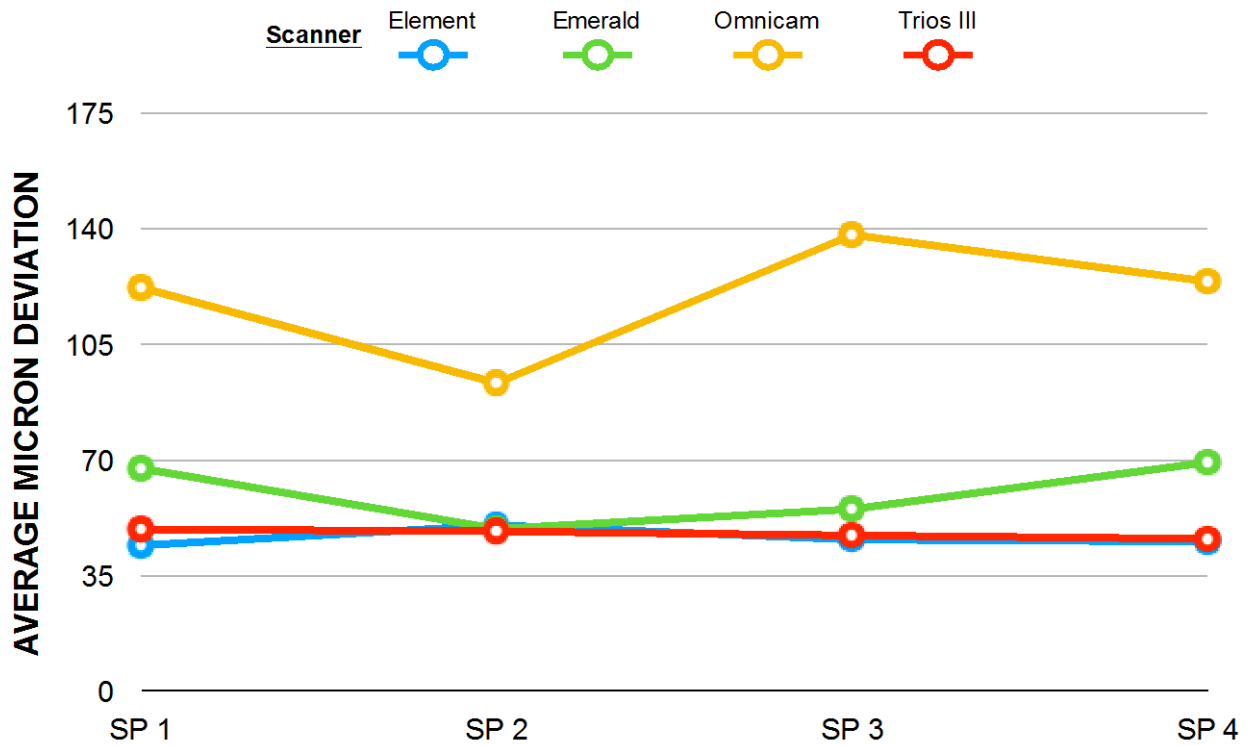
Figure 20. Trueness of scanners within each scan pattern demonstrated. Scanners are represented by color-coded lines. Scan patterns SP1-SP4 are listed on the x-axis. A lower value in microns on the y-axis results in higher trueness. Scan pattern 4 was found to have the greatest number of significant inter-scanner differences. Patterns SP 1, SP 2, and SP 3 each contained 3 significant differences between scanners, where as SP 4 contained 5 significant differences between scanners. The Omnicam scanner was found to have a consistently lower trueness as compared to other scanners within each pattern.

Precision of Scanners Within Scan Patterns

A repeated measures generalized linear model was used with precision as the outcome and scanner in the model. Four models were run, one for each pattern. A random intercept was in the model to account for replicates. Post hoc comparisons for scanner with a Scheffe adjustment were looked at if the main effect was significant. For Pattern 1, the main effect was significant (p-value<0.0001), and the post-hoc comparisons of IE vs CO (p-value=0.0001), PE vs CO (p-value<0.0001) and CO vs TR (p-value=0.0005) and PE vs TR (p-value=0.0191) were all significant. For Pattern 2, the main effect was significant (p-value<0.0001), as were the post-hoc comparisons of IE vs PE (p-value=0.0007), IE vs CO (p-value=0.0002), PE vs CO (p-value=<0.0001), PE vs TR (p-value<0.0001), and CO vs TR (p-value=0.0054). For Pattern 3, the main effect was significant (p-value<0.0001), as were the post-hoc comparisons of IE vs PE (p-value=0.0007, IE vs CO (p-value=<0.0001), IE vs TR (p-value=0.0231), PE vs CO (p-value=<0.0001), PE vs TR (p-value=<0.0001), CO vs TR (p-value=<0.0001). For Pattern 4, the main effect was significant (p-value<0.0001), as were the post-hoc comparisons of IE vs PE (p-value= 0.0105), IE vs CO (p-value=<0.0001), IE vs TR (p-value=0.0048), PE vs CO (p-value=<0.0001), PE vs TR (p-

value=<0.0001), CO vs TR (p-value=<0.0001).   Post-hoc comparisons are

listed in Table 12 with more precise scanners on the left side of the column.

Table 12. Precision significant differences among scanners within scan patterns. Scanners with higher precision are listed on the left.

Scan Pattern 1

Scanner		Scanner	P-value
Element	vs	Omnicam	0. 0001
Emerald	vs	Omnicam	<0. 0001
Trios	vs	Omnicam	0.0005
Emerald	vs	Trios	0.0191

Scan Pattern 2

Scanner		Scanner	P-value
Emerald	vs	Element	0.0007
Element	vs	Omnicam	0.0002
Emerald	vs	Omnicam	<0.0001
Emerald	vs	Trios	<0.0001
Trios	vs	Omnicam	0.0054

Scan Pattern 3

Scanner	vs	Scanner	0.0105
Element	vs	Omnicam	<0.0001
Element	vs	Trios	0.0048
Emerald	vs	Omnicam	<0.0001
Trios	vs	Emerald	<0.0001
Trios	vs	Omnicam	<0.0001

Scan Pattern 4

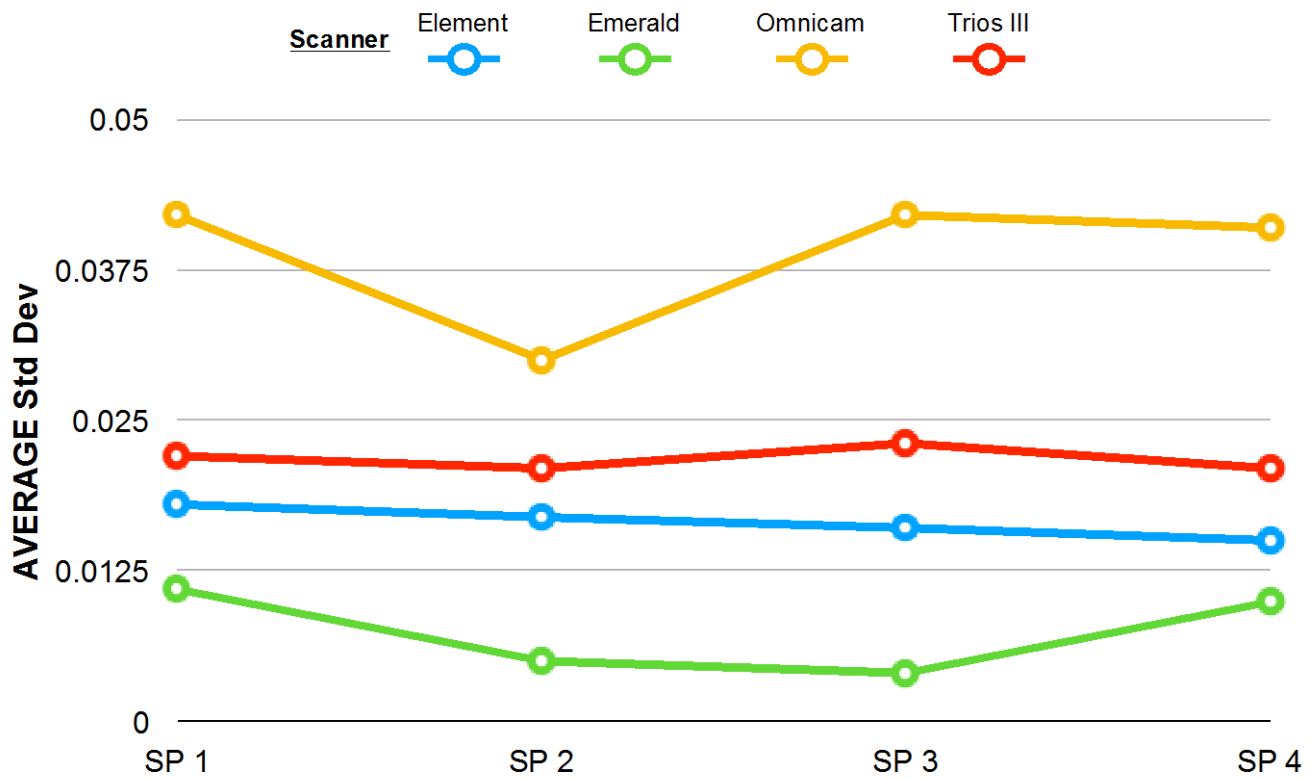| Scanner		Scanner	P-value
Element	vs	Emerald	0.0105
Element	vs	Omnicam	<.0001
Element	vs	Trios	0.0048
Emerald	vs	Omnicam	<.0001
Trios	vs	Emerald	<.0001
Trios	vs	Omnicam	<.0001

Figure 21. Precision of scanners within each scan pattern demonstrated. Scanners are represented by color-coded lines. Scan patterns SP1-SP4 are listed on the x-axis. A large number of significantly different comparisons were found between scanners of each pattern.

Maximum Deviation Comparisons

The absolute values of the maximum and minimum deviations were used to calculate the maximum deviation mean. First, maximum deviation mean values from patterns were compared within each scanner. Mean values were ranked and evaluated for significant differences. Second, maximum deviation mean values from scanners were compared within each pattern. Mean values were ranked and evaluated for significant differences.

Comparing Maximum Deviation Mean Values of Patterns for Each Scanner

Table 13. Maximum deviation means are listed for each scan pattern within scanners. Mean values are listed in microns.

Scanner	Pattern	Max Dev Mean (μm)	Rank
Element	1	408	2
	2	417	3
	3	440	4
	4	380	1
Emerald	1	469	3
	2	418	1
	3	443	2
	4	490	4
OmniCam	1	720	2
	2	610	1
	3	805	4
	4	742	3
Trios	1	484	4
	2	472	1
	3	478	2
	4	483	3

The main effect for CO was found to be significant (p-value=0.0023).

Post hoc comparisons were SP2 vs SP 3 (p-value=0.0027), and SP 2 vs SP 4

(p-value=0.0379).

Table 14. Post hoc comparisons of maximum deviation mean values from
scan pattern within scanners. Patterns with lower mean values listed on the
left.

Omnicam Scanner: p-value=0.0023

Pattern		Pattern	p-value
SP 2	vs	SP 3	0.0027
SP 2	vs	SP 4	0.0379

Maximum Deviation Mean Values for Scanners Within Scan Patterns.

Table 15. Maximum deviation means are listed for each scanner within scan
patterns.

Pattern	Scanner	Mean (μm)	Rank
1	Element	408	1
	Emerald	469	2
	Omnicam	719	4
	Trios	484	3
2	Element	417	1
	Emerald	418	2
	Omnicam	610	4
	Trios	472	3
3	Element	409	1
	Emerald	443	2
	Omnicam	805	4
	Trios	478	3
4	Element	380	1
	Emerald	490	3
	Omnicam	742	4
	Trios	483	2

The main effect for all patterns were found to be significant. For Pattern 1, the main effect was significant (p-value=<0.0001), the post-hoc comparisons included IE vs CO (p-value=<0.0001), PE vs CO (p-value=<0.0001), CO vs TR (p-value=0.0001). For Pattern 2, the main effect was significant (p-value=<0.0001), the post-hoc comparisons included IE vs CO (p-value=<0.0001), PE vs CO (p-value=<0.0001), CO vs TR (p-value=0.0010). For Pattern 3, the main effect was found to be significant (p-value=<0.0001), and the post hoc comparisons included IT vs CO (p-value=<0.0001), PE vs CO (p-value=<0.0001), CO vs TR (p-value=<0.0001). For Pattern 4, the main effect was significant (p-value=<0.0001), the post-hoc comparisons included IE vs PE (p-value=<0.0139), IE vs CO (p-value=<0.0001), IE vs TR (p-value=0.0209), PE vs CO (p-value=<0.0001), CO vs TR (p-value=<0.0001). Post-hoc comparisons are listed in Table 16 with higher trueness on the left of the table.

Table 16. Post-hoc comparisons of maximum deviation mean values. Scanners with lower mean listed on the left.

Pattern 1: p-value=<0.0001

Scanner		Scanner	p-value
Element	vs	Omnicam	<.0001
Emerald	vs	Omnicam	<.0001
Trios	vs	Omnicam	0.0001

Pattern 2: p-value=<0.0001

Scanner		Scanner	p-value
Element	vs	Omnicam	<.0001
Emerald	vs	Omnicam	<.0001
Trios	vs	Omnicam	0.0010

Pattern 3: p-value=<0.0001

Scanner		Scanner	p-value
Element	vs	Omnicam	<.0001
Emerald	vs	Omnicam	<.0001
Trios	vs	Omnicam	<.0001

Pattern 4: p-value=<0.0001

Scanner		Scanner	p-value
Element	vs	Emerald	0.0139
Element	vs	Omnicam	<.0001
Element	vs	Trios	0.0209
Emerald	vs	Omnicam	<.0001
Trios	vs	Omnicam	<.0001

Maximum Deviation Mean Values vs Trueness

Maximum deviation means were compared to trueness in two different ways. First in Figure 29, trueness values of scan patterns within each scanner were illustrated along with maximum deviation mean values. Second, in Figure 30, trueness values of scanners within each scan pattern were compared to mean values of maximum deviation.
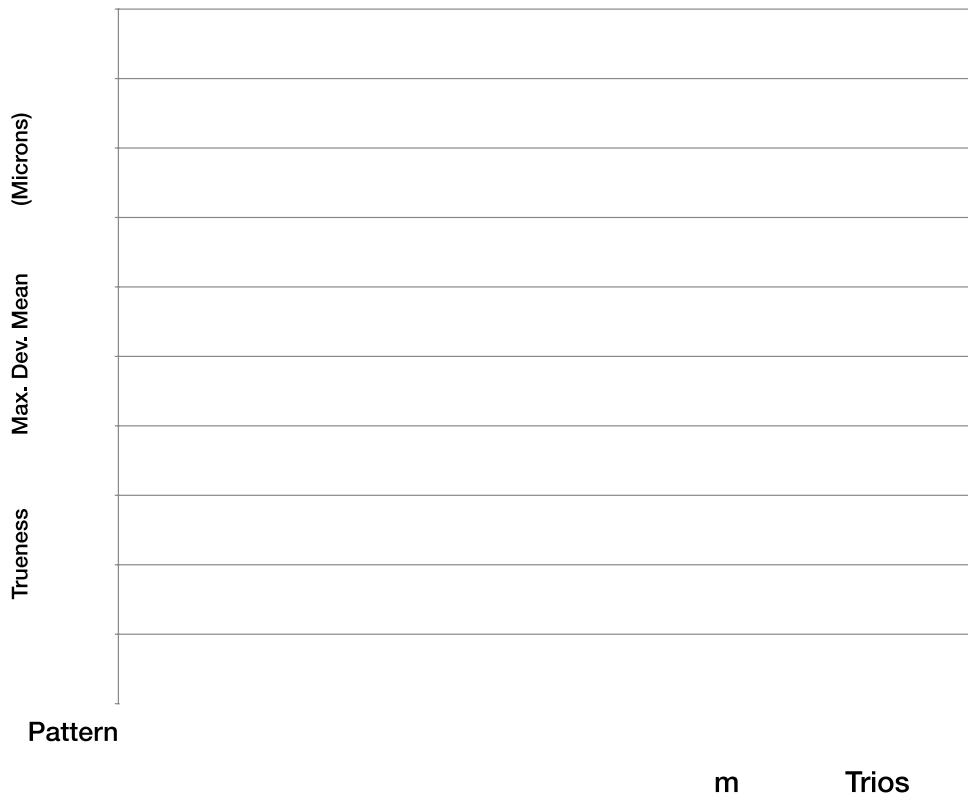

Figure 22. Trueness values of scan patterns within each scanner illustrated along with maximum deviation mean values. Significant differences were noted between CO and IE, PE, and TR Scanners.

65

Scanner Trueness vs Maximum Deviation Mean Values Within
Each Pattern

anner

Pattern

Figure 23. Trueness of scanners within each scan pattern compared to each other along with mean values of maximum deviation.

3D Compare Image Analysis

  Custom views were taken from the Geomagic Control X *3D Compare* function and grouped by scanner and numbered according to their scan order. The software's color bar (Figure 13) was set at a range of +/-500 μm with darker red colors indicating positive, or outward deviations and darker blue colors indicating negative, or inward deviations between the test and reference model. Color deviation was analyzed among scans and patterns were highlighted.
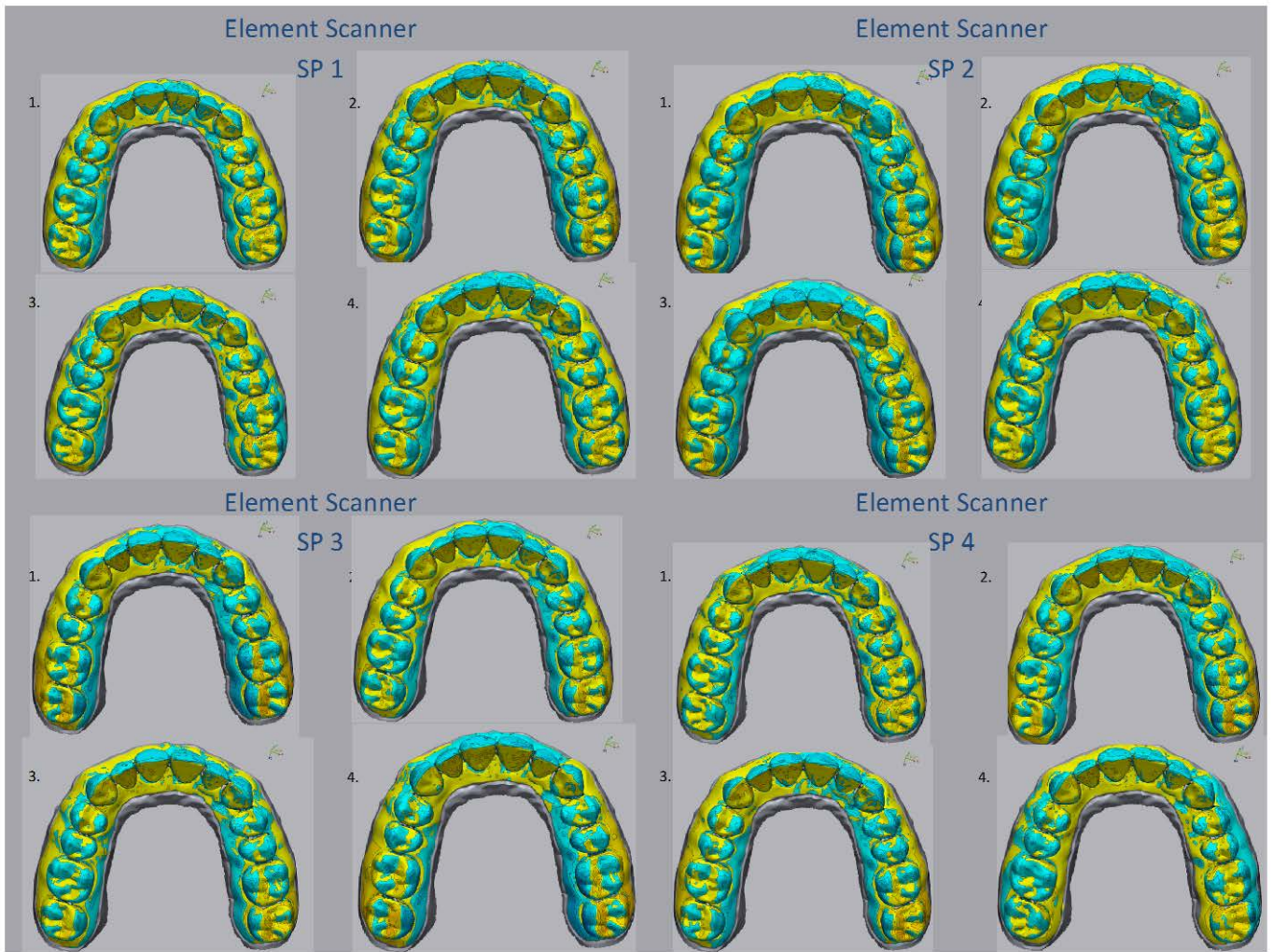
Figure 24. Element scanner *3D Compare* Images ranked in order of which they were taken. Scan patterns from left to right include SP 1, SP 2, SP 3, and SP 4. Generally, a small amount of constriction of the facial surfaces were noted on incisors, as well as posterior palatal constriction. Buccal posterior soft tissue showed a small amount of expansion.
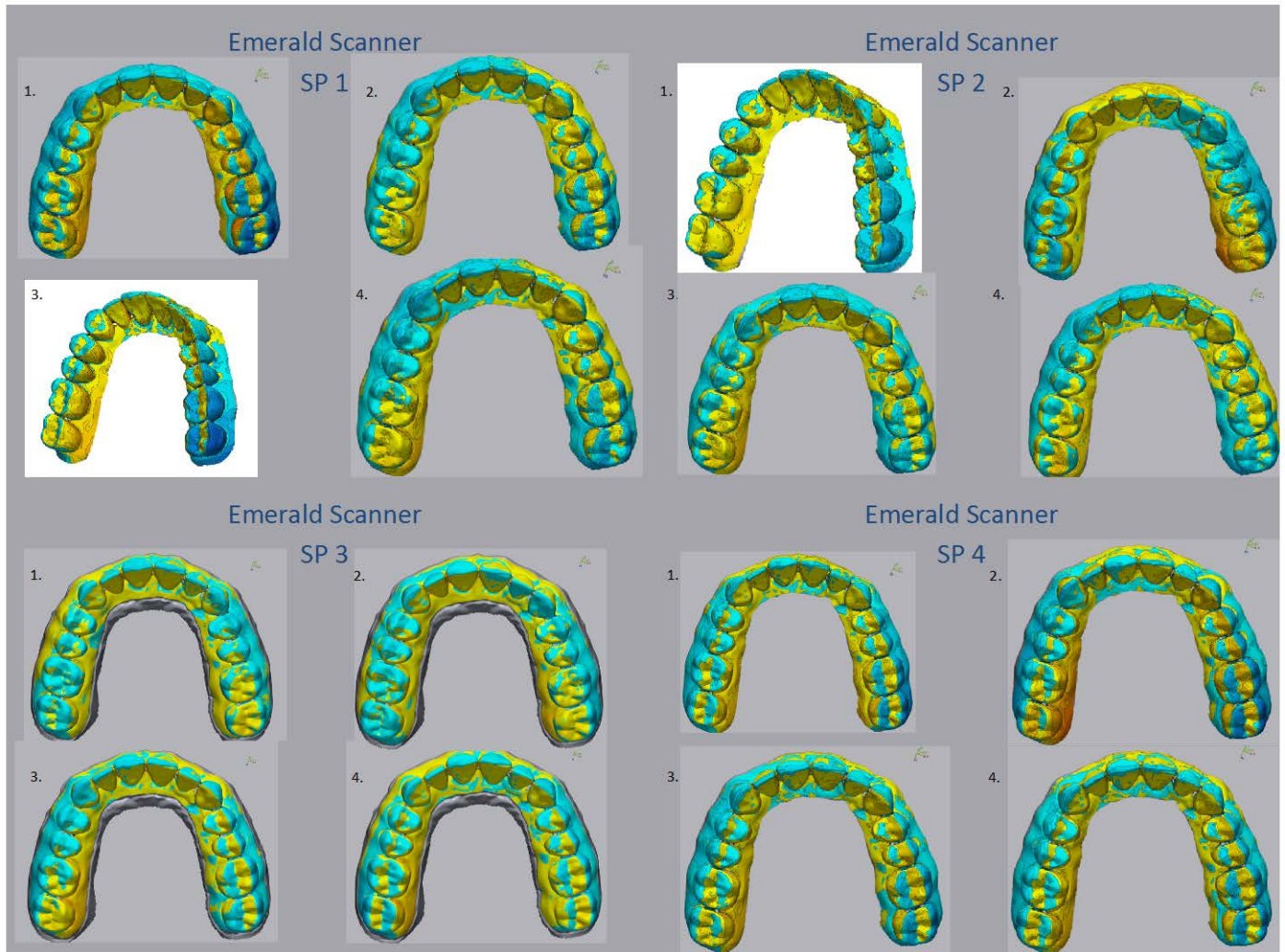
Figure 25. Emerald scanner *3D Compare* Images ranked in order of which they were taken. Scan patterns from left to right include SP 1, SP 2, SP 3, and SP 4. Patterns SP 1, SP 2 and SP 4 showed posterior buccal constriction more pronounced than SP 3. Posterior palatal expansion was noted on a small number of scans from SP 1, SP 2 and SP 4. Generally, color changes were more uniform on SP 3, where as SP 1, SP 2, and SP 4 showed unique variations from one another.
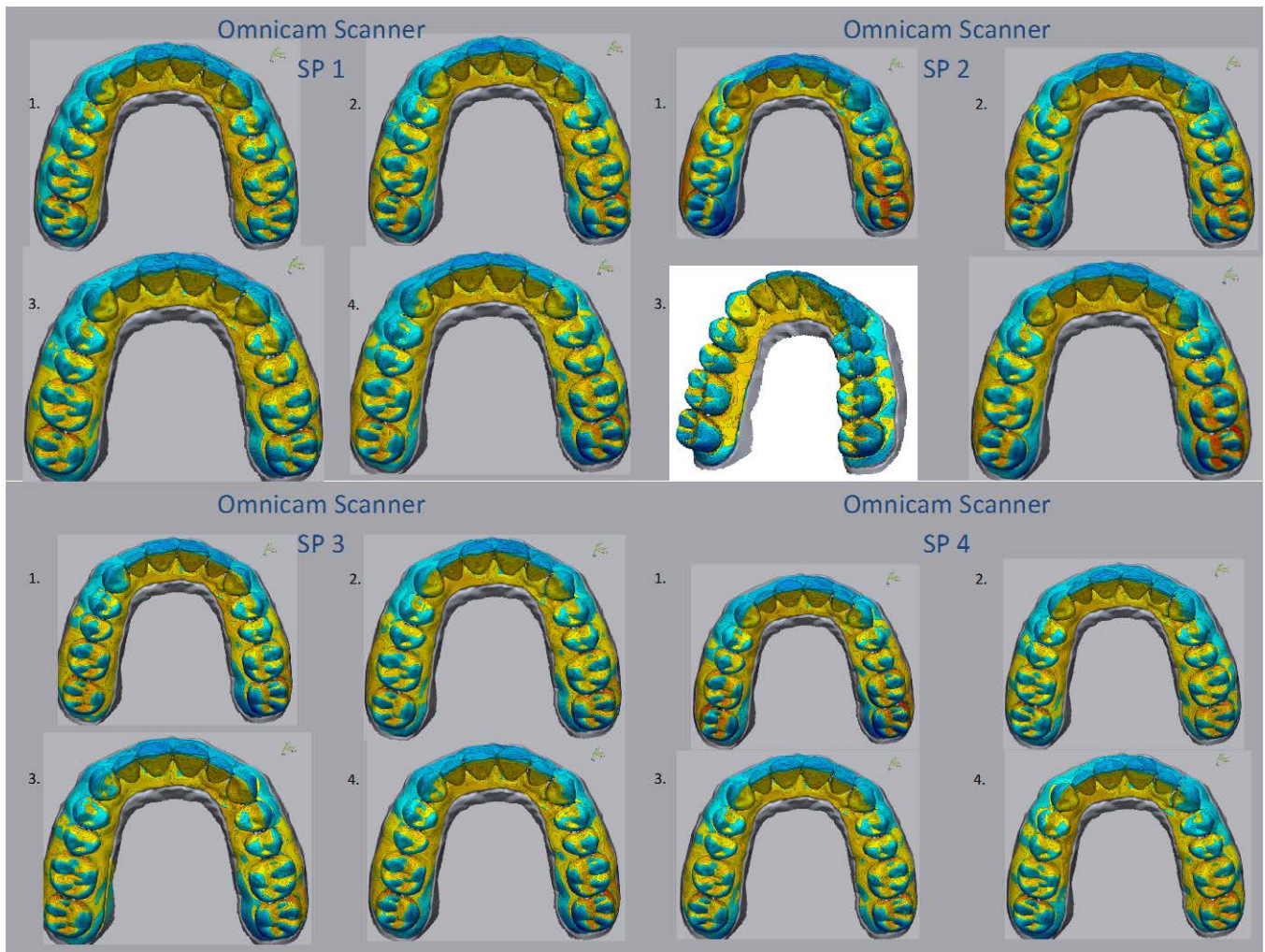
Figure 26. Omnicam scanner *3D Compare* Images ranked in order of which they were taken. Scan patterns from left to right include SP 1, SP 2, SP 3, and SP 4. CO scans generally showed posterior constriction on the palatal surfaces of the terminal molars and anterior facial constriction from the first

premolar to contralateral first premolar. SP 2 showed a slight amount of expansion of the facial surface of the lingual cusps on the left terminal molars. A slight amount of constriction of the facial surface of the lingual cusps on the contralateral terminal molars was noted.

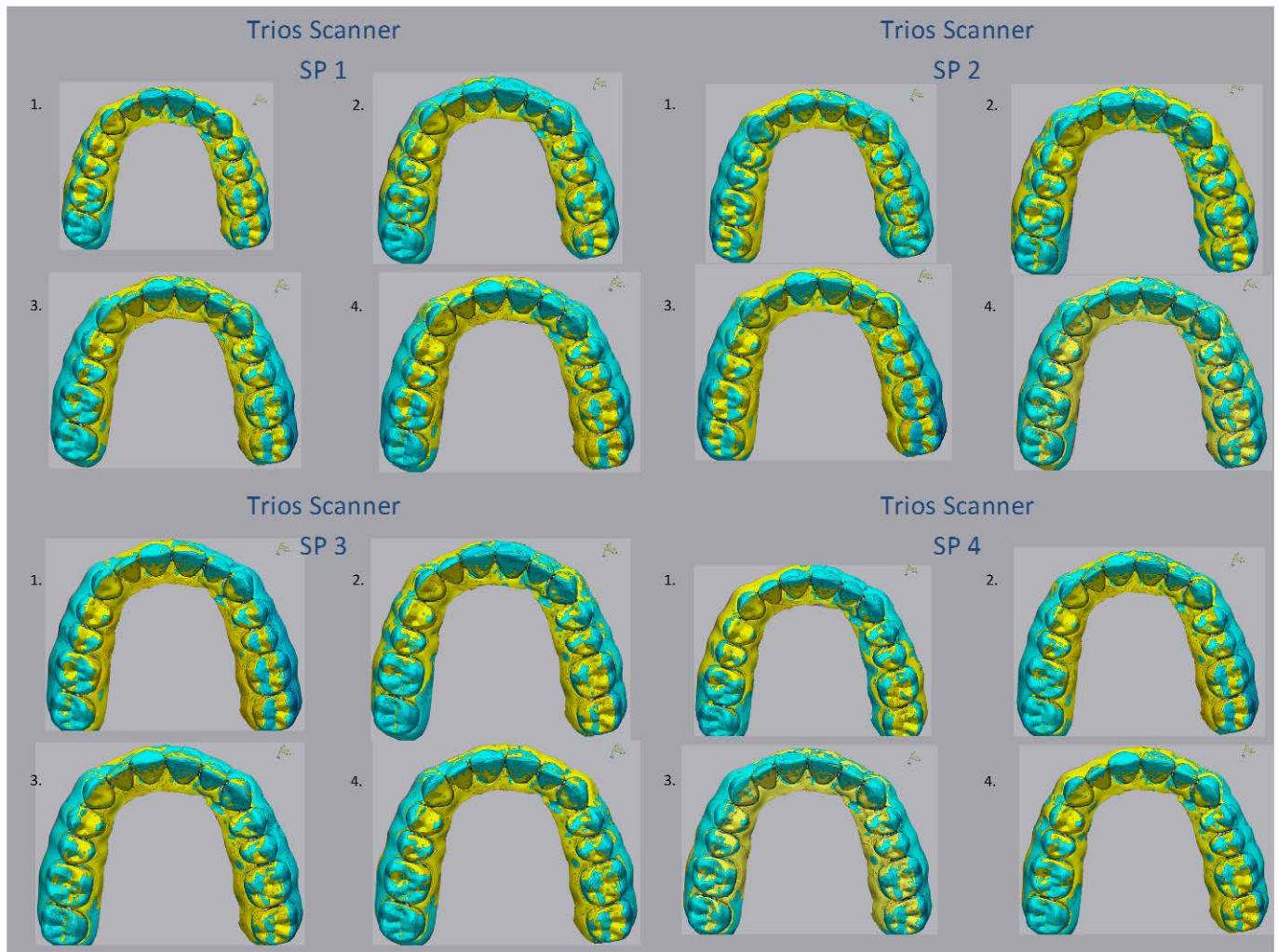**Figure 27.** Trios III scanner *3D Compare* images ranked in order of which they were taken. Scan patterns from left to right include SP 1, SP 2, SP 3, and SP 4. Color mapping of the TR IOS showed generally similar color mapping amount all patterns. Facial surfaces of the anterior teeth were slightly constricted, along with buccal surfaces of posterior teeth. Palatal surfaces of posterior teeth showed slight positive deviation.

Discussion

To examine the influence of scan strategies on IOS accuracy, overall scanner trueness and precision comparisons were completed. Overall pattern trueness and precision comparisons were also done. This was followed by an evaluation of the significant differences in scanners within each scan pattern, and scan patterns for each scanner. Evaluating scanners within each pattern allowed for observation of inter-scanner discrepancies within each pattern used. Evaluation of patterns within each scanner allowed for evaluation of discrepancies between patterns used on the same scanner. Maximum deviation mean values were also evaluated and checked for significant discrepancies between scanners and patterns. Finally, a visual inspection was completed using the Geomagic *3D Compare* results to evaluate trends in color changes, which could be compared to trueness and precision results.

Overall scanner comparisons revealed that the tested IOS system trueness values ranged from 46 μm to 119 μm. Scanners ranked from most true to least true as follows: IE>TR>PE>CO. Significant differences in trueness were found between all scanners except IE vs TR. Overall precision

findings showed scanners ranked from most precise to least precise as follows: PE>IE>TR>CO. Significant differences in precision were found between all scanners (p-value=<0.0001). Study design, device hardware and software make comparison of the study results to previous literature difficult, but a few studies reported findings on similar IOS devices. A previous finding from a systematic review on scanner accuracy noted full arch deviation findings of less than 100 μm on several newer scanners such as the TR and CO[20]. Another study reported full arch trueness of 69.6 μm on the TR, and 107.6 μm on the CO[10].

Overall scan pattern comparisons revealed that patterns ranked from most true to least true as follows: SP 2> SP 1> SP 4> SP 3. No significant differences were noted in trueness between overall pattern comparisons (p-value=0.7365). Overall pattern precision showed that patterns ranked from most precise to least precise as follows: SP2>SP3>SP4>SP1. No significant precision differences were found between overall patterns (p-value=0.6587). No significant scan time differences were noted between overall scan patterns (p-value=0.0987).

The null hypotheses that scan strategies do not affect trueness and precision was partially rejected. This was due in part to several of the scan patterns showing significant differences in trueness within the CO scanner

74

(p-value=0.0019). The IE, PE, and TR systems showed no significant

differences in trueness between scan patterns tested on each system.

Precision was mixed when comparing patterns for each scanner, and

also lead to a partial rejection of the null hypothesis. The PE and TR scanners

showed no significant differences in precision with changes in scan

strategies, where as the main effect for the IE (p-value=0.0307), and CO (p-

value=0.0026) scanners was significant for several scan patterns.   These

findings contrasted slightly with the visual analysis of the *3D Compare* output

in that the PE scanner showed color mapping variability between several

scan patterns (Figure 25).

The null hypothesis was accepted for scan times and their effects on

trueness and precision. No significant differences were noted when scan

time was set as a covariant with precision or trueness.   These findings

suggest that scan time had no appreciable effect on accuracy within the

study. That said, significant inter-system scan time differences were found

between all scanners except the CO vs PE.   Significant differences in scan

times were noted between scan patterns within the IE, PE, and CO systems. A

previous study by Renne et al, which evaluated the accuracy of 7 digital

scanners, noted a correlation between scan time with trueness, and scan time

with precision in full arch scans. The study used one desktop scanner and 6

IOS scanners, two of which were the CO and TR[10]. A review by Rutkunas et al also suggested a correlation between scan time and accuracy [20].

Maximum deviation analysis showed that although all of the scanners are highly accurate on average, maximum deviations of between 380-805 μm occurred. Inter-system deviations were found to be significant, with the CO scanner showing the highest deviation (805 μm). When comparing maximum deviation values of patterns within each scanner, the PE, IE, and TR systems showed no significant variation, where as the CO scanner had significant variation between several patterns.

Visual analysis of the IE scanner showed very little variation, but some overall findings were noted. A small amount of constriction was noted on the facial surfaces of the incisors, as well as posterior palatal constriction. Buccal posterior soft tissue showed a small amount of expansion.

Visual analysis of the PE scans showed posterior palatal expansion on a small number of scans from SP 1, SP 2 and SP 4. Generally, color changes were more uniform on SP 3, where as SP 1, SP 2, and SP 4 showed unique variations from one another.

Visual analysis of the CO scans showed posterior constriction on the palatal surfaces of the terminal molars and anterior facial constriction from the first premolar to contralateral first premolar. SP 2 showed a slight

amount of expansion of the facial surface of the lingual cusps on the left

terminal molars. A slight amount of constriction of the facial surface of the

lingual cusps on the contralateral terminal molars was noted.

Visual analysis of the TR scans showed generally similar color

mapping among all patterns. Facial surfaces of the anterior teeth were

slightly constricted, along with buccal surfaces of posterior teeth. Palatal

surfaces of posterior teeth showed slight positive deviation.

Overall, visual analysis of the scanners revealed a pattern of negative

incisor facial surface deviation on all scans. Posterior color mapping changes

were more uniform in the TR and IE scanners, although statistically the TR

and PE were found to be the most precise between scan patterns. An in vivo

study by Nedeclu et al showed similar incisor deviation findings. The study

tested the accuracy of 3 IOS systems and completed a visual analysis of scans

from the CO, TR, and 3M True Definition (3M, St. Paul, USA)[59]. Their

findings showed that the TR scanner had higher trueness and precision than

the CO scanner. The study reported that all of the tested scanners showed

positive posterior deviations in the premolar area, as well as negative facial

deviations on incisors[59].

Similarly to other studies evaluating IOS accuracy, this study has

many limitations. First and foremost, this study was performed under non-

clinical conditions, without the influence of intraoral blood, saliva, soft tissue

variation, or presence of various types of dental materials[9]. Although the

scanners used may be the same as previously tested, software versions may

differ thus potentially making accuracy comparisons difficult[9, 20].

Conclusion

The rapid pace of digital impression system technology in orthodontics can be daunting to keep up with. New scanners and software upgrades are released frequently with claims of accuracy that must be verified to be as accurate or more accurate than conventional impression methods[23]. Previous studies have shown that many variables can affect the accuracy of IOS systems such as hardware, software versions, characteristics of objects scanned, clinical factors such as saliva and soft tissue, experience of the operator, and scanning protocol and strategy[20, 56].

This study examined full arch scan strategies on a custom made dental typodont. The primary aim of the study was to determine whether scan strategy has an effect on IOS device trueness and precision. A secondary aim was to illustrate whether scan time has any effect on trueness and precision.

In the present study, 3 of the scanners showed no significant differences in trueness with changes in scan patterns. Conversely, the CO scanner showed statistically significant differences in trueness between different scan patterns. The IE and CO scanners showed statistically significant variations in precision with changes in scan patterns, but their

clinical relevance could be called into question due to the small degree of variation. Additionally, scan times showed no statistically significant impact on trueness or precision, although there were significant inter-scanner differences.

Maximum deviation mean values were relatively high in several scanners, which warrants further research in determining how much of the model is at or near the maximum deviation ranges, and where the deviation locations are within the test model.

The presented findings highlight the need for continued research with intraoral scanners and scan strategies. In addition, in vivo conditions would be ideal to better replicate clinical conditions.

References

1.   Kravitz, N.D., et al., *Intraoral digital scanners.* J Clin Orthod, 2014. 48(6): p. 337-47.
2.   Ahlholm, P., et al., *Digital versus conventional impressions in fixed prosthodontics: a review.* Journal of Prothodontics, 2016 : p. 1-5
.
3.   Jacob, H.B., G.D. Wyatt, and P.H. Buschang, *Reliability and validity of intraoral and extraoral scanners.* Prog Orthod, 2015. 16: p. 38.
4.   Martin, C.B., et al., *Orthodontic scanners: what's available?* J Orthod, 2015. 42(2): p. 136-43.
5.   Jung, Y.R., et al., *Accuracy of four different digital intraoral scanners: effects of the presence of orthodontic brackets and wire.* Int J Comput Dent, 2016. 19(3): p. 203-15.
6.   Guth, J.F., et al., *A new method for the evaluation of the accuracy of full-arch digital impressions in vitro.* Clin Oral Investig, 2016. 20(7): p. 1487-94.
7.   Ender, A. and A. Mehl, *Influence of scanning strategies on the accuracy of digital intraoral scanning systems.* Int J Comput Dent, 2013. 16(1): p. 11-21.
8.   Standardization, I.O.f., *Accuracy (trueness and precision) of measurement methods and results* in *Part 1: General principles and definitions.* 1997: Berlin: Beuth Verlag GmbH.
9.   Francesco FG, V.G., Hauchild U, Mijirisky C, *Trueness and Precision of Four Intraoral Scanners in Oral Implantology: A Comparative in Vitro Study.* PLoS One, 2016 . 11(9).
10.   Renne, W., et al., *Evaluation of the accuracy of 7 digital scanners: An in vitro analysis based on 3-dimensional comparisons.* J Prosthet Dent, 2017. 118(1): p. 36-42.
11.   Muller, P., et al., *Impact of digital intraoral scan strategies on the impression accuracy using the TRIOS Pod scanner.* Quintessence Int, 2016. 47(4): p. 343-9.
12.   Gary D. Hack, S.B.M.P., *Evaluation of the Accuracy of Six Intraoral Scanning Devices: An in-vitro Investigation.* ADA Professional Product Review, 2015. 10(4): p. 5.

13. Nedelcu R, P.A., *Scanning accuracy and precision in 4 intraoral scanners: an invitro comparison based on 3-dimensional analysis.* J Prosthet Dent, 2016. 112: p. 1461-71.

14. Bohner, L.O.L., et al., *Computer-aided analysis of digital dental impressions obtained from intraoral and extraoral scanners.* The Journal of Prosthetic Dentistry, 2017
. 118(5): p. 617-623.

15. Yang, X., et al., *Accuracy of digital impressions and fitness of single crowns based on digital impressions.* Materials (Basel), 2015. 8(7): p. 3945-3957.

16. Su T, S.J., *Comparison of repeatability between intraoral digital scanner and extraoral digital scanner: an in-vitro study.* J Prosthet Dent, 2015. 59
: p. 236-242.

17. Mennito, A.S., et al., *Evaluation of the effect scan pattern has on the trueness and precision of six intraoral digital impression systems.* J Esthet Restor Dent, 2018.

18. Richert, R., et al., *Intraoral Scanner Technologies: A Review to Make a Successful Impression.* J Healthc Eng, 2017. 2017: p. 8427595.

19. Logozzo, S., et al., *Recent advances in dental optics: part I: 3D intraoral scanners for restorative dentistry.* Optics and Laser Engineering, 2013. 54: p. 203-221.

20. Rutkunas, V., et al., *Accuracy of digital implant impressions with intraoral scanners. A systematic review.* Eur J Oral Implantol, 2017. 10 Suppl 1: p. 101-120.

21. Park, J.M., et al., *Impact of Orthodontic Brackets on the Intraoral Scan Data Accuracy.* Biomed Res Int, 2016. 2016: p. 5075182.

22. Mangano, F., et al., *Intraoral scanners in dentistry: a review of the current literature.* BMC Oral Health, 2017. 17(1): p. 149.

23. Goracci, C., et al., *Accuracy, reliability, and efficiency of intraoral scanners for full-arch impressions: a systematic review of the clinical evidence.* Eur J Orthod, 2016. 38(4): p. 422-8.

24. Glenner, R.A., *Dental impressions.* J Hist Dent, 1997. 45(3): p. 127-30.

25. Guerini, V., *A history of dentistry*. 1909, Philadelphia and New York: Lea and Febiger.

26. Glenner, R., *How it evolved: dental impressions* in *Chairside Magazine*.

27. Harris, C., *The dental art, practical treatise on dental surgery*. Classics of Dentistry Library edition. 1839: Baltimore.

28. Polido, W.D., *Digital impressions and handling of digital models: The future of Dentistry.* Dental Press Journal of Orthdontics, 2010. 15(5): p. 18-22.

29. Olitsky, J., *Digital impressioning making its way into dentistry's mainstream.* Compend Contin Educ Dent, 2012. 33(9).

30. Peluso, M.J., Josell, S.D., Levine, S.W., Lorei, B.J., *Digital models: an introduction.* Semin Orthod, 2004. 10.

31. Demajo, J.K., et al., *Effectiveness of Disinfectants on Antimicrobial and Physical Properties of Dental Impression Materials.* Int J Prosthodont, 2016. 29(1): p. 63-7.

32. Kotsiomiti, E., A. Tzialla, and K. Hatjivasiliou, *Accuracy and stability of impression materials subjected to chemical disinfection - a literature review.* J Oral Rehabil, 2008. 35(4): p. 291-9.

33. Sofou, A., et al., *In vitro study of transmission of bacteria from contaminated metal models to stone models via impressions.* Clin Oral Investig, 2002. 6(3): p. 166-70.

34. Thongthammachat, S., et al., *Dimensional accuracy of dental casts: influence of tray material, impression material, and time.* Journal of Prothodontics, 2002. 11(2): p. 98-108.

35. Yuzbasioglu, E., et al., *Comparison of digital and conventional impression techniques: evaluation of patients' perception, treatment comfort, effectiveness and clinical outcomes.* BMC Oral Health, 2014. 14: p. 10.

36. Burhardt, L., et al., *Treatment comfort, time perception, and preference for conventional and digital impression techniques: A comparative study in young patients.* Am J Orthod Dentofacial Orthop, 2016. 150(2): p. 261-7.

37. Hacker, T., G. Heydecke, and D.R. Reissmann, *Impact of procedures during prothodontic treatment on patients' perceived burdens.* J Dent, 2015. 43(1): p. 51-57.

38. Rossini, G., et al., *Diagnostic accuracy and measurement sensitivity of digital models for orthodontic purposes: A systematic review.* Am J Orthod Dentofacial Orthop, 2016. 149(2): p. 161-70.

39. Birnbaum, N., et al., *3D digital scanners: a high-tech approach to more accurate dental impressions.* Inside Dentistry, 2009. 5(4).

40. Duret, F., *Empreinte optique*, in *Faculté d odontologie thèse*. 1973.

41. Ruthwal, Y., et al., *Digital impressions: a new era in prosthodontics.* Journal of Dental and Medical Sciences, 2017. 16(6): p. 82-84.

42. Mörmann, W., *The evolution of the cerec system.* JADA, 2006. 137(9): p. 7-13.

43. Mindksy, M., *Microspocy apparatus*, U. Patent, Editor. 1961: USA.
44. Pawley, J., *Handbook of biological confocal microscopy*. 3rd ed. 2006, New York: Springer.
45. Aragon, M.L., et al., *Validity and reliability of intraoral scanners compared to conventional gypsum models measurements: a systematic review.* Eur J Orthod, 2016. 38(4): p. 429-34.
46. Vecsei, B., et al., *Comparison of the accuracy of direct and indirect three-dimensional digitizing processes for CAD/CAM systems - An in vitro study.* J Prosthodont Res, 2017. 61(2): p. 177-184.
47. Ender, A. and A. Mehl, *Accuracy of full arch dental impressions, a new highly accurate method of measuring trueness and precision.* J Prosthet Dent, 2013. 109: p. 121-128.
48. Belser, U.C., M.I. MacEntee, and W.A. Richter, *Fit of three porcelain-fused-to-metal marginal designs in vivo: a scanning electron microscope study.* J Prosthet Dent, 1985. 53(1): p. 24-9.
49. *Planmeca user manual*, D.D.T. LLC, Editor. 2017: Richardson, TX.
50. Imburgia, M., et al., *Accuracy of four intraoral scanners in oral implantology: a comparative in vitro study.* BMC Oral Health, 2017. 17(1): p. 92.
51. Lee, B., et al., *Evaluation of the fit of zirconia copings fabricated by direct and indirect digital impression procedures.* J Prosthet Dent, 2018.
52. *iTero Website*. http://www.itero.com/en-us.
53. Rosenstiel SF, L.M., Fujimoto J., *Contempoary fixed prosthodontics*, in *Contemporary fixed prosthodontics*, 5th, Editor. 2016, Mosby/ Elsevier: St. Louis. p. 325.
54. Janiszewska-Olszowska, J., et al., *Three-dimensional quantitative analysis of adhesive remnants and enamel loss resulting from debonding orthodontic molar tubes.* Head Face Med, 2014. 10: p. 37.
55. Dold, P., et al., *Validation of an optical system to measure acetabular shell deformation in cadavers.* Proc Inst Mech Eng H, 2014. 228(8): p. 781-6.
56. Lim, J.H., et al., *Comparison of digital intraoral scanner reproducibility and image trueness considering repetitive experience.* J Prosthet Dent, 2018. 119(2): p. 225-232.
57. Low, K.-L., *Linear least-squares optimization for point-to-plane ICP surface registration*. 2004, University of North Carolina, Chapel Hill.
58. Marani, R., Reno, V., Nitti, M., D'Orazio, T., Stella, E. , *A modified iterative closest point algorithm for 3D point cloud registration.* Computer- Aided Civil and Infrastructure Engineering, 2016. 31: p. 515-534.

59.   Nedelcu, R., et al., *Accuracy and precision of 3 intraoral scanners and accuracy of conventional impressions: A novel in vivo analysis method.* J Dent, 2018. 69: p. 110-118.